TALLINNA TEHNIKAÜLIKOOL
TALLINN UNIVERSITY OF TECHNOLOGY

Thomas Johann Seebeck Department of Electronics

Methodology and setup for investigation of the influence of breathing on the heart rate variability.

Master's Thesis

Submitted by

Recai Mert Erdil

Supervisor: Paul Annus

Tallinn, 2015

Table of Contents

Page

Abbrevations iv

List of Figures v

Acknowledgements vii

Abstract viii

1. Introduction 1

2. Theory 3

2.1 Electrical Impedance 3
2.2 Bio-Impedance 4
2.3 Breathing 7
2.4 Heart-Rate Variability 7
2.5 Influence of breathing on HRV 9

3. Method 10

3.1 Setting Up the Experiment 10
3.1.1 Components 10
3.1.1.1 Impedance Spectroscope 10
3.1.1.2 Switchbox and electrodes 12
3.1.1.3 Spirometer 14
3.1.2 Setup 15
3.2 Data Acquisition 15
3.3 Processing Data 16

4. Results and Discussion 20

5. Conclusions 25

References: 26

Appendix A: MATLAB codes for implementation 27

Appendix B: Obtained Data 31

Abbrevations

BI	Bio-Impedance
EBI	Electrical Bio-Impedance
ECG	Electro Cardiography
HPF	High Pass Filter
ICG	Impedance Cardiography
IRG	Impedance Respirography
FIR	Finite Impulse Response
IIR	Infinite Impulse Response
LPF	Low Pass Filter
TD	Tidal Volume
VC	Vital Capacity
HR	Heart Rate
VR	Ventilation Rate

List of Figures

Figure 1: Representation of impedance in complex plane 3

Figure 2: Formation of the electrical bioimpedance of the tissue[3] 5

Figure 3:High and low frequency current paths through tissue 5

Figure 4: ECG, Bioimpedance (Z) and its derivative plotted simultaneously [12] 6

Figure 5: Basal(Z_0) and modulated(ΔZ) components of Z[4] 6

Figure 6: Front and back view of Zurich Instruments HF2IS 10

Figure 7: Screenshot from LabView program used for controlling ZI HF2IS 11

Figure 8: A sample of block diagram of LabView program for Impedance Spectroscope 12

Figure 9:Front and back view of Electrode Switchbox 12

Figure 10: Screenshot from the LabView program controlling the Switchbox 13

Figure 11: A sample of block diagram of LabView program for the switchbox 13

Figure 12:Spirometer used in the experiments[10] 14

Figure 13: Setup for the experiments 15

Figure 14: Detecting R peaks manually 17

Figure 15: Grid generated by makegrid.m 17

Figure 16: ECG signal plotted with the grid generated by ecgcomp.m 18

Figure 17: Comparison of ΔZ / Z0 values 19

Figure 18: Heart rate between adjacent heartbeats 19

Figure 19: Real part, imaginary part and magnitude of Z at 30 kHz, respectively 20

Figure 20: Few possible candidates for the next R peak 21

Figure 21: Ambiguous position of R peak and examination of the exact location from impedance 22

Figure 22: Respiration signal and running average over 2000 points 23

Figure 23: Correlation of bioimpedance and respiration 23

Figure 24: Heart rate (continuous) and respiration (dashed) 24

Figure 25: Magnitude of Z for 1, 3, 5 and 8 kHz, respectively 31

Figure 26: Magnitude of Z at 5, 7, 9 and 11 kHz, respectively 32

Figure 27: Magnitude of Z at 9, 13 and 15 kHz, respectively 33

Figure 28: Magnitude of Z at 20, 25 and 30 kHz, respectively 34

Figure 29: Magnitude of Z at 35, 40 and 45 kHz, respectively 35

Figure 30:Real part, imaginary part and magnitude of Z at 1kHz 36

Figure 31:Real part, imaginary part and magnitude of Z at 5 kHz 37

Figure 32:Real part, imaginary part and magnitude of Z at 10kHz 38

Figure 33:Real part, imaginary part and magnitude of Z at 15 kHz 39

Figure 34: Real part, imaginary part and magnitude of Z at 20 kHz 40

Figure 35:Real part, imaginary part and magnitude of Z at 25 kHz 41

Figure 36: Real part, imaginary part and magnitude of Z at 30 kHz 42

Figure 37: Real part, imaginary part and magnitude of Z at 35 kHz 43

Figure 38: Real part, imaginary part and magnitude of Z at 40 kHz 44

Figure 39: Real part, imaginary part and magnitude of Z at 45 kHz 45
Figure 40: Real part, imaginary part and magnitude of Z at 50 kHz 46

Acknowledgements

I would like to express my gratitude to my advisor in Tallinn University of Technology, Dr. Paul Annus, for his guidance, suggestions and supports throughout this research. Also I would like to extend my appreciation to my friends, my colleagues for their valuable support and fellowship.

I am forever indebted to my family who have been supporting me in every aspects of life.

Abstract

In this thesis, a setup for acquisition of respiratory and cardiac activity via bioimpedance is implemented with the purpose of investigation of the relationship in between. Heart rate variability is a phenomenon that is still being investigated by scientists, and it is thought that breathing has influence on it. The method implemented on this thesis shows that information related to both are present in the electrical bioimpedance (EBI) data, though a method of successful separation is needed.

Key Words: Heart-rate variability, Electrical bio-impedance

1. Introduction

Bioimpedance was primarily measured with the intention of estimating the water and electrolyte content, as well as physiological variables such as thyroid function, basal metabolic rate and blood flow in tissues.[1]. Today, accurate measurement of biological materials and tissues over a broad frequency range provides valuable information of different kinds. Below are some examples to bioimpedance applications:

- Dental research
- Monitoring the extendt of tissue damage and organ integrity for transplants
- Detection and study of tumors
- In-vivo (alive and functioning) testing of muscle and tissues
- Dermatological applications
- Drug delivery rates
- Blood cell analysis
- Biotechnology research [2]

In addition, thoracic electrical bioimpedance (EBI) is known to include information about cardiac activity and respiration. This puts it in a unique position for investigation of the relationship in between. Even though methods for accurate acquisition of these data are still in process of being developed, EBI is seen as a promising method.

One such relationship being investigated is the influence of breathing on the heart rate variability (HRV). HRV is a valuable diagnostic tool for certain pathologies, and usually requires recordings of cardiac data for extended amounts of time (e.g, 24 hours). Including the respiratory information to examine the influence is not very convenient for the patient. EBI presents an opportunity for minimizing this inconvenience.

Since EBI appears to be a promising method for investigation of the influence of breathing on the heart rate variability, a setup for acquisition of cardiac and respiratory information will be proposed and examined in this thesis.

The following chapter includes basic concepts about impedance, bioimpedance, respiration and heart-rate variability are given to familiarize the reader with the concepts.

Third chapter starts with introducing the components, which the setup is established with. The next section provides details about how the components are put together. Afterwards, data acquisition is briefly explained, and on the last section the processing of acquired data is explained.

Results are presented on fourth chapter

In the last chapter of the thesis, author's conclusions are included.

2. Theory

2.1 Electrical Impedance

Electrical impedance is the amount of opposition that a material presents to current or voltage change. It is a complex quantity, consisting of a real part (R) and imaginary part (X). Real part R is known as resistance and imaginary part X as reactance. So the electrical impedance is represented as:

$$Z = R + jX$$

it can be visualized if we use a plane consisting of two axes. Let's name the horizontal axis as Re for real part and the vertical axis as Im for imaginary part. Impedance itself, therefore will represent a vector in this so-called "complex plane" which starts at origin and ends in point Z which is R units to the right of origin, and X units to the top.

For practical purposes, it is often needed to know how far away from the origin this point is. This is called the magnitude of the impedance, and is shown as |Z|. To differentiate the point Z from all the other points which are |Z| units away from the origin, we need to know another property of Z. The directional angle between the horizontal (Re) axis and the vector will do nicely. We will refer to this angle as the "phase". Below, there is a figure visualizing the attributes of impedance that are just explained.

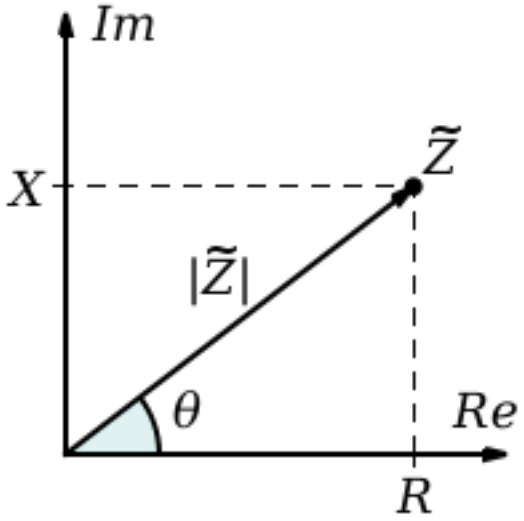

Figure 1: Representation of impedance in complex plane

A few fundamental trigonometric and geometric relations are apparent in this figure, for

example the real and imaginary parts can be calculated as amplitude multiplied by the cosine and sine of the angle, respectively. Likewise, obtaining the magnitude and the phase is quite easy.

In numerical terms, it is the complex ratio of the voltage to the current in an alternating current (AC) circuit. Magnitude of the impedance corresponds to ratio of magnitudes of voltage to current, and phase corresponds to the amount that voltage leads or lags the current.

There are three important types of elements in AC circuits. Impedance of resistive elements is real, capacitive and inductive elements are purely imaginary with phase angles -90° and +90°, respectively. All of the real and passive RLC circuits, which consist of arbitrary combination of the above mentioned elements, have therefore their representative impedance vector on the right side of the complex plane between phase angels -90° and +90°. Obviously different combinations of resistive, inductive and capacitive elements yield different impedances. It is important to note that the position and the magnitude of the impedance vector are generally frequency dependent.

There is also a fourth type of elements worth mentioning – so-called memristors, which link changes in magnetic flux and charge. It is generally however considered that memristive and inductive behavior can be safely ignored in the case of the impedance of materials of biological origin and therefore they will not appear in the frames of the current thesis.

2.2 Bio-Impedance

Biological tissues can be thought as combinations of resistive and capacitive elements. In this sense, when excited with an AC current, an AC voltage appears across the tissue. Bio-impedance can be defined as the complex ratio of the voltage across the tissue to the excitation current passing through the tissue. Different parts of the tissue show different characteristics, i.e. cells are both capacitive and resistive, whereas fluid between cells (extracellular fluid) is mostly resistive. [3]

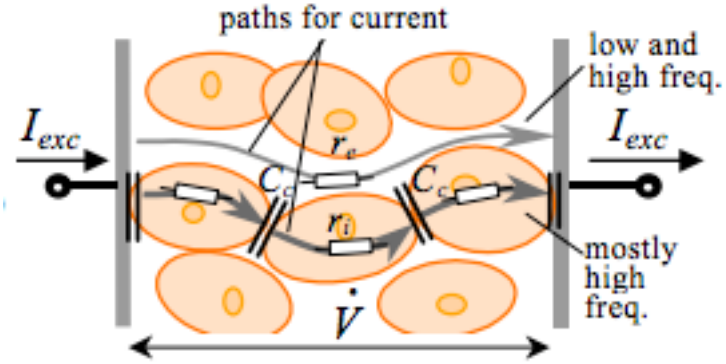

Figure 2: Formation of the electrical bioimpedance of the tissue[3]

As a corollary, bioimpedance is also dependent on frequency. Intracellular path is the only available route for very low frequency or DC currents, whereas high frequency currents have considerably more routes to flow, since capacitive impedance is easily overcome with sufficiently high frequencies.

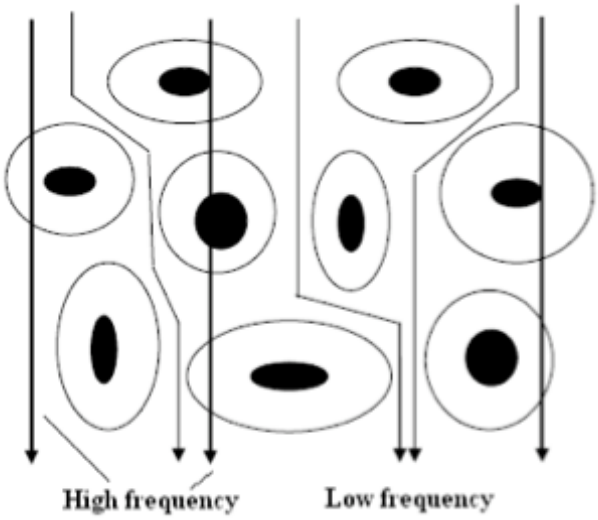

Figure 3:High and low frequency current paths through tissue

Also, state of the tissue is also an important factor. There are many complicated factors that determine the bioimpedance. Change of length of a cell due to deformation or muscular contraction, introduction of air between cells (e.g around the lungs), electrical activity in nerve cells, varying flow of fluids (e.g. blood in veins) are some examples that are continuously going on in healthy organisms.

One very important such contributor for the purpose of this thesis is the heart beat. When plotted on top of each other, the relationship between bioimpedance and ECG is

apparent. As can be seen in figure 4, bioimpedance is in its lowest value around the R peak of ECG signal. Its derivative is also negative for a short duration afterwards. With this information, it can be expected to see negative dips in bioimpedance signal near the locations of R peaks.

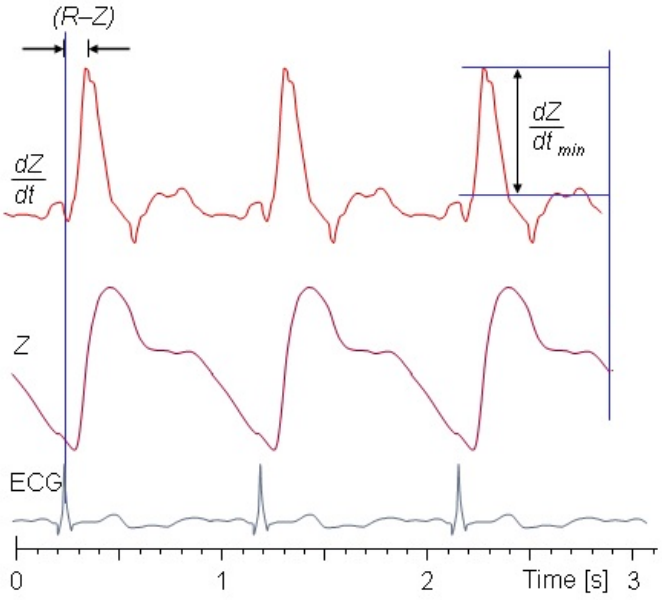

Figure 4: ECG, Bioimpedance (Z) and its derivative plotted simultaneously [12]

For convenience, total bioimpedance (Z) will be defined as the combination of two complex parts. Z_0 is the basal part of bioimpedance and ΔZ is the small variations in time, modulated on Z_0.

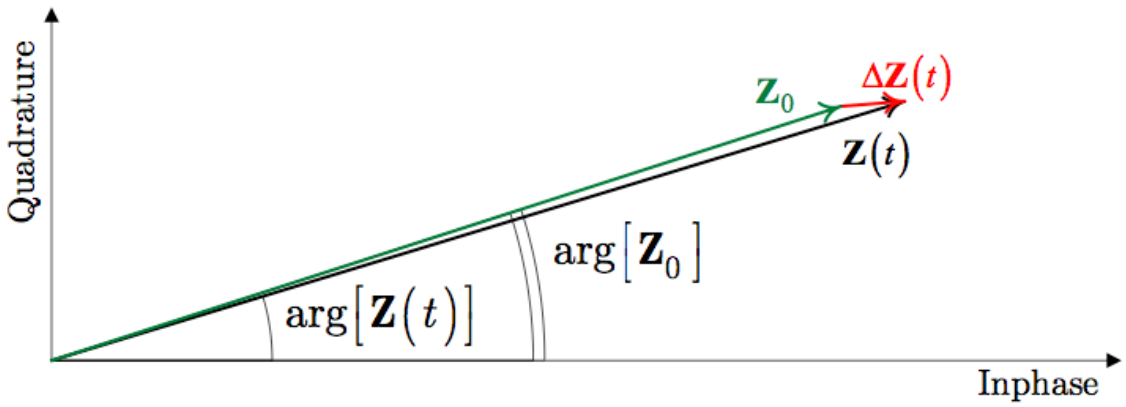

Figure 5: Basal(Z_0) and modulated(ΔZ) components of Z[4]

In this regard, if ΔZ is very small in magnitude relative to Z_0, extracting needed

information would be very hard. Therefore, it is a good idea to look for the ratio $\Delta Z / Z_0$ to be as high as possible.

2.3 Breathing

Breathing is one of the defining actions of a living organism. Human life could be viewed as beginning with the first breath, and ends with the last one. It is of vital importance in both direct (i.e. supplying fresh air rich in oxygen to the organism) and indirect ways, therefore has great diagnostic value.

It is easily noticeable that the lungs are not fully inflated in every inhalation and fully deflated in every exhalation. Humans usually breathe on a fixed interval, i.e. there is usually an inspiratory and an expiratory reserve volume on the lungs (IRV and ERV). Also there is always some volume the lungs cannot go below. This is referred to as residual volume (RV). The interval between IRV and ERV, where people normally breathe is called tidal volume (TV). On the data we use over the course of this thesis, it is assumed that all breathing is within the boundaries of TV.

As inhalation introduces air into the lungs, and since air is not a very good conductor, it is logical to expect the inhalation to introduce a significant increase to the capacitive component. It can be thought as increasing the distance between the plates of a capacitor.

2.4 Heart-Rate Variability

Electrocardiogram (ECG) signal is the first thing that comes to mind when a person thinks about anything related to heart. The repetitive beeping of an electrocardiograph is thought to be an indication of a healthy person. This establishes a conception that steadier the ECG, healthier the person. Heart-rate variability (HRV) is the variation of the duration between consecutive heartbeats. In other words, it is the exact opposite of a steadily beating heart. Apparently, steadier heartbeats (low HRV) have direct correlation to mortality [5].

Beat to beat intervals are sometimes referred to as NN (normal to normal) intervals, and this is usually measured between r peaks of the QRS complex.

There are different methods for measuring the HRV and interpreting the results. Firstly, ECG signal is recorded for a fixed period of time; 5 minutes and 24 hours are typical values for short term and long term. While long term recordings are capable of collecting data during different states such as sleeping, resting, light exercise; short term recordings are preferred in stationary conditions. Interpretation methods can be grouped in 3 categories: Time domain, frequency domain and non-linear methods.

For stationary short term recordings, frequency domain measures are preferred, since more theoretical knowledge and experience exist on physiological interpretation. Both time domain and frequency domain variables match when long term recordings are considered, and since it allows easier identification of physical processes and is easier to perform, time domain methods are usually preferred unless a parameter specific to frequency domain is of interest. [6]

Other than simple time domain variables like NN intervals (duration between consecutive heart beats), mean heart rate and difference between longest and shortest NN intervals; statistical and geometrical methods are employed to determine different variables. Typical parameters of statistical methods include parameters obtained directly from NN intervals such as SDNN (Standard deviation of NN intervals on the long term. This is also the square root of variance) and SDANN (standard deviation of average of NN intervals on the short term); and ones obtained from the differences between successive NN intervals such as RMSSD (RMS value of standard deviation of differences between successive NN intervals), NN50 (number of NN intervals greater than 50 milliseconds), pNN50 (ratio of NN50 to total number of NN intervals). With geometrical methods, first geometrical patterns are constructed with various methods (such as histograms of the NN intervals or difference between successive NN intervals, Lorenz plots of NN intervals etc.) and than parameters of these constructed patterns are obtained.[6]

For frequency domain methods, firstly bands of frequencies are determined and than the number of NN intervals corresponding to these bands are counted. After this, the parameters about the probabilistic distributions of heart rate are attempted to be obtained either by making strong assumptions about the shape of the probabilistic structure (i.e. parametric methods), or without assuming a fixed model (i.e. non-

parametric models. Parametric methods have advantages like smoother spectral components, easy post-processing and accurate estimation even with small samples; whereas non-parametric methods provide high processing speed and usually use simple algorithms like fast Fourier transform. [6]

2.5 Influence of breathing on HRV

There are various studies examining the reasons and influencing factors of HRV. One of the most influential appears to be breathing.

HRV depends on both the depth and the frequency of the breathing. When the tidal volume is kept constant, HRV is high and relatively stable for low breathing frequencies. As the frequency increases, after a certain frequency HRV first peaks and then drops as much as 20 dB per decade. At approximately half the frequency as that of the peak, a dip was also reported.[7]

HRV is also found to exhibit similar frequency response characteristics with different tidal volumes. Even though the shape is similar, HRV increases with increased tidal volumes. [7]

One interesting fact is that, especially in low frequencies, after a while of breathing with fixed frequency, when the breath is hold with a certain amount of volume inside the lungs, amplitude of HRV is similar to equivalent tidal volume. This means that even though HRV is influenced directly by lung volume, it is not relevant how this volume is achieved. This implies that neurological activity for breathing is not the origin of HRV and does not dictate its amplitude. [7]

3. Method

3.1 Setting Up the Experiment

In this section, first the components will be introduced, than the setup will be explained.

3.1.1 Components

3.1.1.1 Impedance Spectroscope

Figure 6: Front and back view of Zurich Instruments HF2IS

Suitable for static and dynamic impedance spectroscopy, Zurich Instruments HF2IS has two differential measurement units with a wide frequency range and 4 dual-phase demodulators, which are matched with the unprecedented precision of a 128-bit DSP engine. This permits to perform multi-frequency measurements with very high sensitivity and precise static impedance characterization combined in one fully digital bench top instrument. These capabilities satisfy the highest impedance measurement requirements of leading research laboratories. Key features include:

- 2 measurement units with single-ended and differential operation
- 0.7 µHz - 50 MHz analog frequency range
- 210 MSa/s, 14 bit A/D conversion
- 4 frequencies simultaneously
- 2/3/4-terminal measurement configurations

- Large range of demodulation filter settings
- 4x 1 MSa/s, 16 bit, ±10 V auxiliary analog output
- 2x 400 kSa/s, 16 bit, ±10 V auxiliary analog input
- USB 2.0 high-speed host connection [8]

Even though the impedance spectroscope has it's own control software, a custom built LabView program was used. This program was developed by Eliko and TUT Thomas Johann Seebeck Department of Electronics staff. Below are some screenshots of the program as in panel view and block diagram

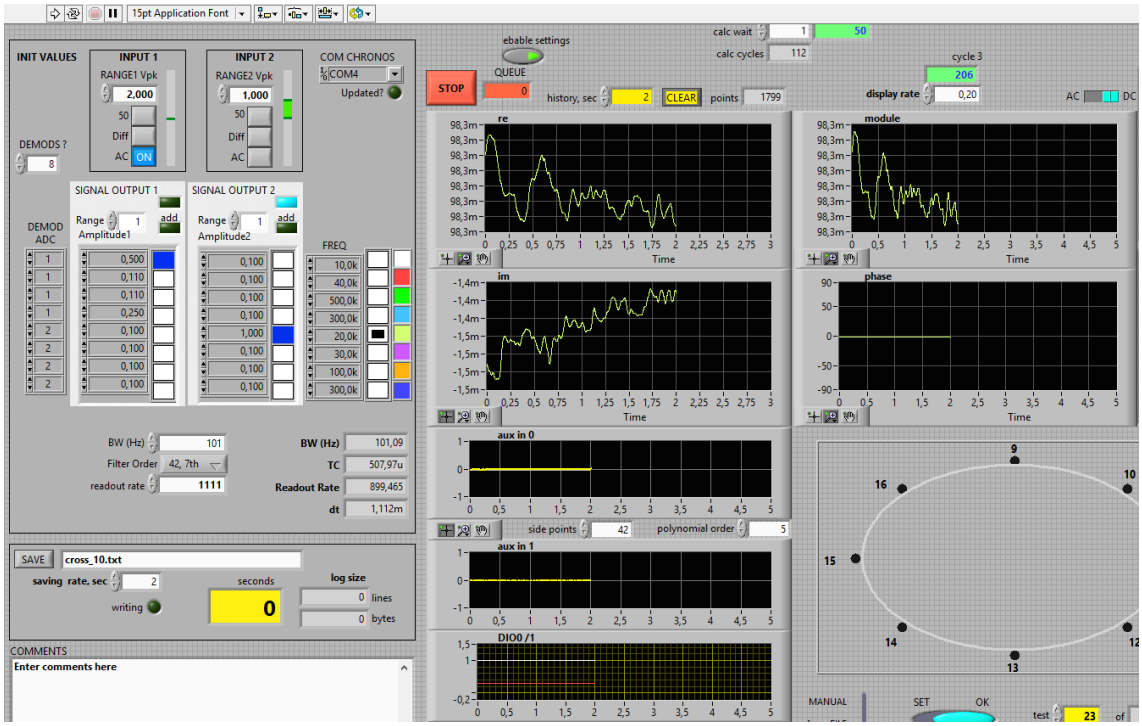

Figure 7: Screenshot from LabView program used for controlling ZI HF2IS

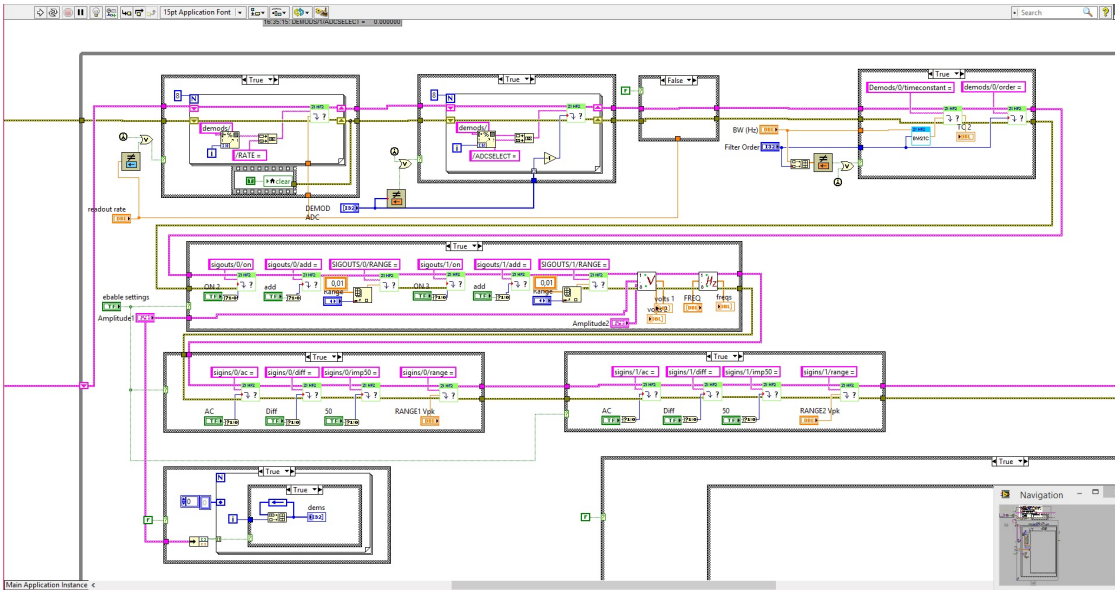

Figure 8: A sample of block diagram of LabView program for Impedance Spectroscope

3.1.1.2 Switchbox and electrodes

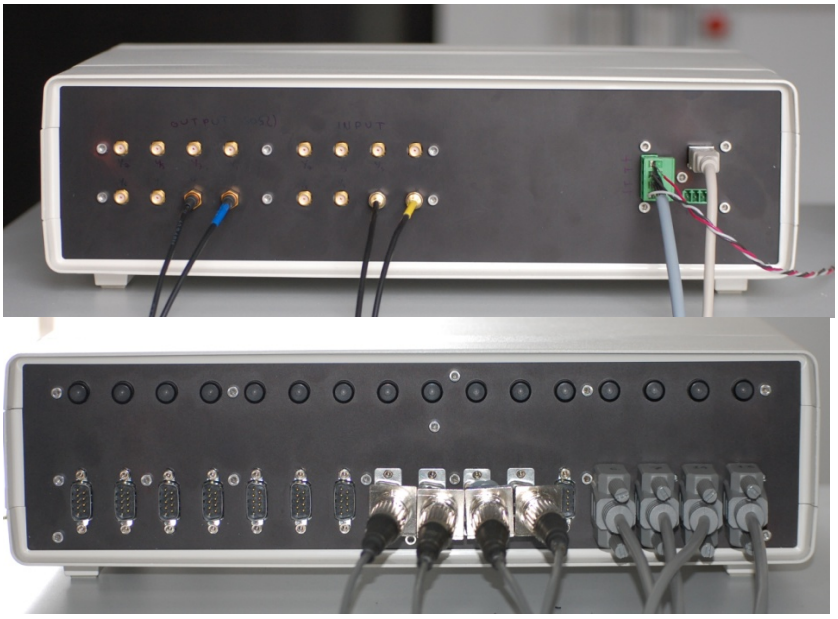

Figure 9:Front and back view of Electrode Switchbox

Since TUT Thomas Johann Seebeck Department of Electronics has extensive experience in bioimpedance field, a switchbox has been developed and built by the staff. Having 16 input output (I/O) sockets on the back, 4 differential input and 4 differential output ports on the front panel, which can be interconnected arbitrarily, this switchbox handles different electrode configurations. It communicates with computer via a USB port, and A LabView program have also been developed to control the

configuration. Screenshots from the program are shown in following figures.

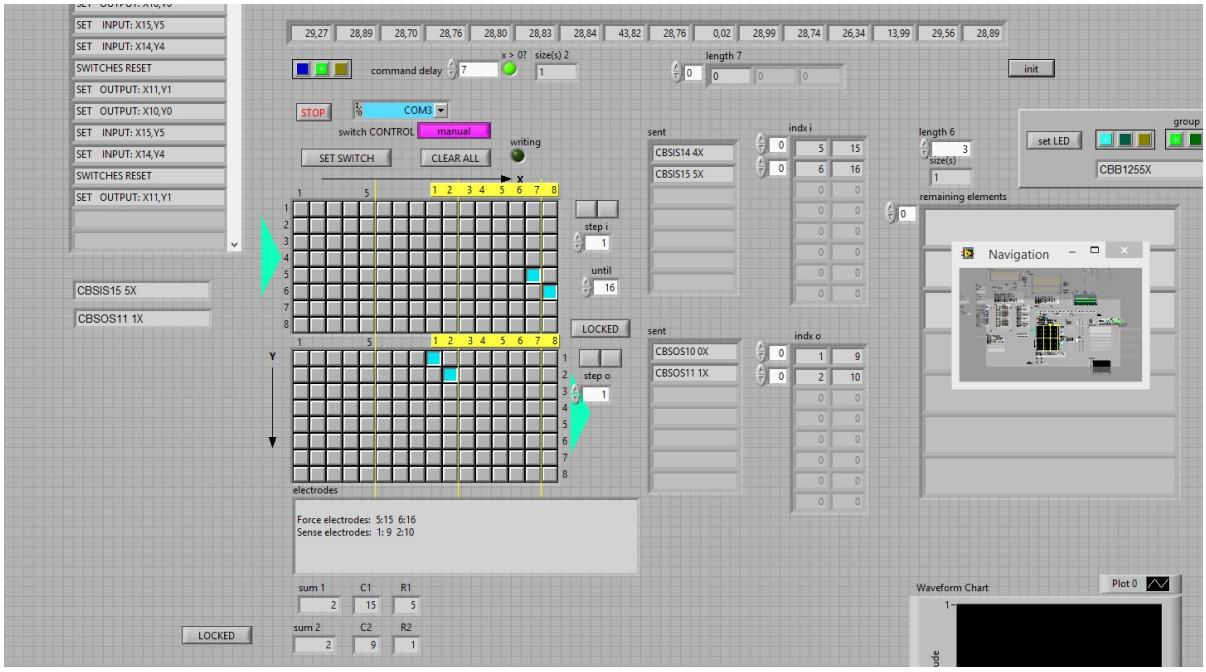

Figure 10: Screenshot from the LabView program controlling the Switchbox

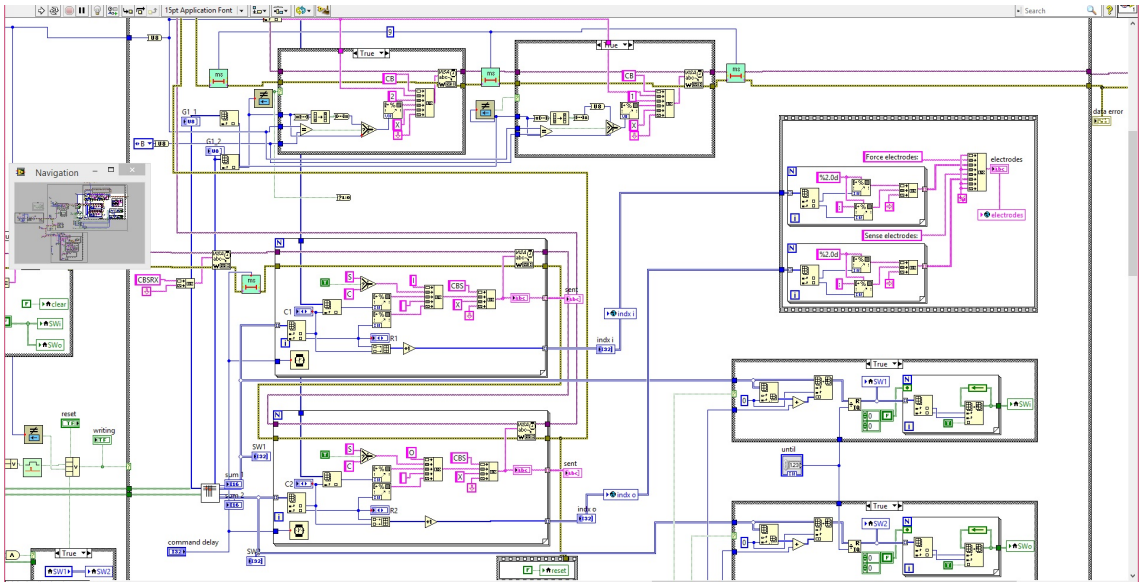

Figure 11: A sample of block diagram of LabView program for the switchbox

3.1.1.3 Spirometer

Figure 12:Spirometer used in the experiments[10]

Since it is desired to acquire breathing information from the bioimpedance measurement, it is important to acquire the information separately to validate the findings. For this reason, a spirometer that has been developed by a fellow master's degree student has been used.

The spirometer has 2 photo detectors, each giving a pulse when the blade passes them, so one leads the other for inhalation and vice versa for exhalation[10]. The LabView program controlling the impedance spectroscope also extracts data output from this device. In the Matlab script extractfifth, these output pulses are processed and breathing information is obtained.

3.1.2 Setup

The experiment is set up with above main components (and some other generic components such as power supplies, oscilloscopes etc) in the way shown in the figure.

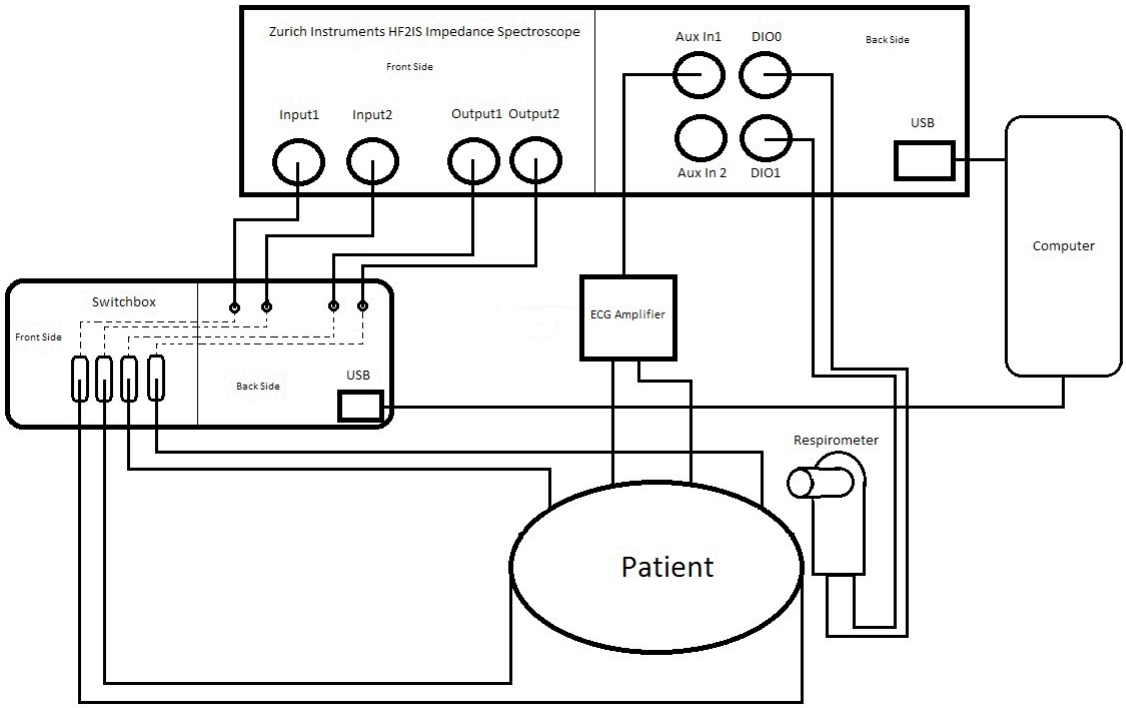

Figure 13: Setup for the experiments

One of the most crucial considerations in this setup is the electrode placement on the subject's body. It is obvious that electrodes for bioimpedance measurement should be close to lungs and heart, but for the best results, a high impedance change to lung volume change linearity is important. The best possible outcome for this is obtained when one set of electrodes are placed between biceps brachii and medial head of triceps brachii on either side; and the other set is placed just outside of pectoralis major muscle. [11]. ECG data is monitored conventionally, with an electrode on each hand connected to an amplifier.

3.2 Data Acquisition

ZI can multiplex up to 8 frequencies into a single signal and plot the impedance data with respect to each frequency accordingly. During this experiment, firstly a few sets of data are taken with multiple frequencies to find the best ratio of $\Delta Z / Z_0$. Afterwards, since the noise would be reduced, the measurements at the frequency of the best found

ratio of $\Delta Z / Z_0$ are done one by one without introduction of any other signal of another frequency.

Frequencies Scanned

- 1 kHz
- 5 kHz
- 10 kHz
- 15 kHz
- 20 kHz
- 25 kHz
- 30 kHz
- 35 kHz
- 40 kHz
- 45 kHz
- 50 kHz

The LabView program that is used to operate the ZI also filters the output.

3.3 Processing Data

Here, the methodology for acquiring raw data and processing it is explained. All functions explained here can be found on chapter Appendix A.

The LabView program for ZI outputs a MS Excel file with headers, ECG data, spirometer data, timestamps and both real and imaginary parts of the impedance in 8 channels. The file is manually cropped and simplified to only have relevant data.

After this, data is handled in Matlab environment. Simplified Excel file is imported into a matrix using xlsread command.

For beginning, since 3 or 4 channels are multiplexed, a Matlab function editdata.m is written to extract timestamp and ECG data, and calculate magnitude of each channel.

After this, ECG data is plotted, and positions of R peaks are noted. Since different processes in thorax contribute to the output signal, and most notably the leakage from 50 Hz mains is superimposed on top of this mixture, ECG signal collected between opposite hands have some noise on it. This noise, in some measurements, prevented the

automatic calculation of heartbeat intervals. Since R peaks are the easiest portions of the ECG data to identify, their locations are noted with the help of data cursor.

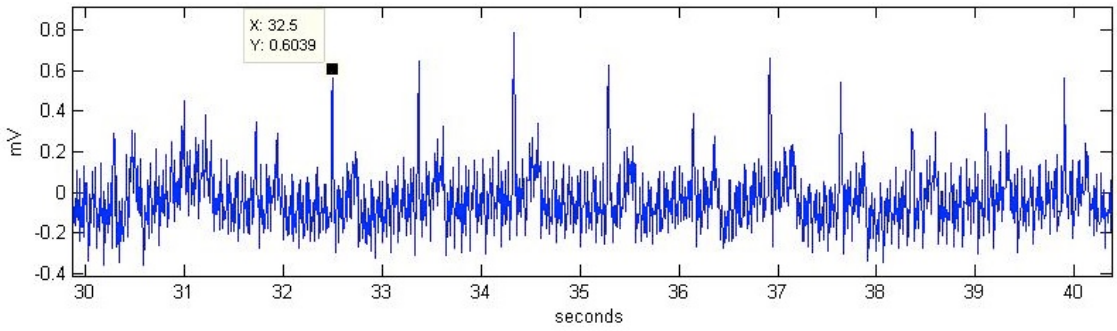

Figure 14: Detecting R peaks manually

These peaks are then fed as input to the function makegrid.m. This function outputs a vector called grid, which has value 1 on the point where there is an R peak in ECG signal and zero elsewhere. The motivation for this is that we are only interested in rough locations of heartbeats for evaluating the impedance data.

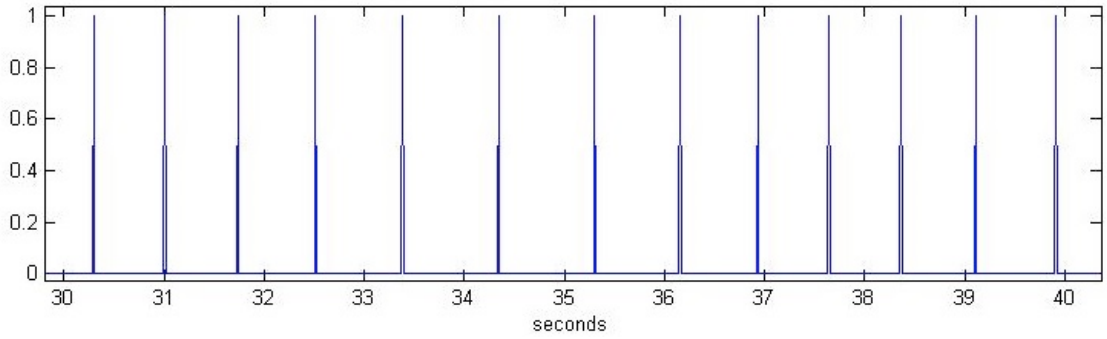

Figure 15: Grid generated by makegrid.m

The next step is to plot the data of our choice with heartbeats shown in the same graph. For this, a Matlab function called ecgcomp is written. Below is a figure showing the output of the function with the ECG signal itself as the input.

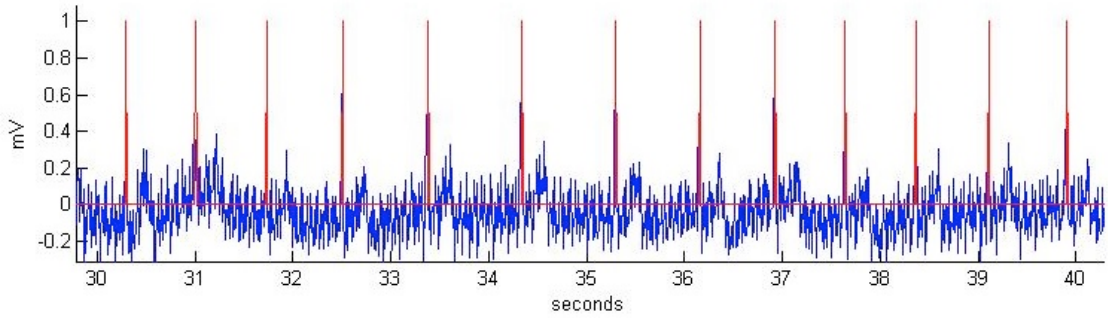

Figure 16: ECG signal plotted with the grid generated by ecgcomp.m

As mentioned in section 3.2, after these data are processed and plotted, a whole new set of data is collected. For this new set of data, a more detailed version of editdata is created as extractfifth. We set the injecting current from the fifth channel of ZI's output, hence the name. This function only deals with one set of impedance data (i.e, only a pair of two vectors for real and imaginary parts, rather than 8 pairs) and it extracts real part, imaginary part and magnitude of the impedance, as well as ECG, breathing, timestamp data and prints out the frequency.

After this, the ecgcomp function is improved to include breathing data and calculate the $\Delta Z / Z_0$ ratio. Breathing data is calculated simply by comparing two channels of pulses of respirograph; total volume is increased or decreased by a unit when one pulse leads or lags the other one. For $\Delta Z / Z_0$ ratio, a running average with a window of 40 is calculated throughout the signal and then rms value of the difference between this running average and the sample itself is calculated to estimate ΔZ. Rms value of the whole signal is calculated to estimate Z_0. These values are than divided to obtain an approximate $\Delta Z / Z_0$ value. The motivation for this is that while the most efficient frequency is picked, it is preferred this value to be as high as possible. Following table compares these values across used frequencies and real parts, imaginary parts and magnitudes.

f	Re	Im	Mag
1 kHz	0.00024628	0.014146	0.00079374
5 kHz	0.00027231	0.0032901	0.00027109
10 kHz	0.00024628	0.0022097	0.00024372
15 kHz	0.00028685	0.0019587	0.00028199
20 kHz	0.00023213	0.0014497	0.00022949
25 kHz	0.00021772	0.0011436	0.0002126
30 kHz	0.00018776	0.00093834	0.00018727
35 kHz	0.00018597	0.00080021	0.00018019
40 kHz	0.0002114	0.0010234	0.0002107
45 kHz	0.00016418	0.00066316	0.00015979
50 kHz	0.00016885	0.00066444	0.00016655

Figure 17: Comparison of ΔZ / Z0 values

As can be seen from the table, there is no value that stands out from others, therefore this information does not help with picking a frequency.

For the next step, same data is collected with selected frequency, only for a duration of 5 minutes. For this, the data rate is reduced from 1000 to 100 samples per second to reduce the total number of samples. This introduced some noise to ECG data, causing inconveniences while picking the R peaks.

Representation of the respiration is also affected by reducing the sampling rate. When plotted on its own, a decreasing and then significantly increasing trend is visible, as well as a waveform resembling a triangular shape instead of a sinusoidal one.

For better visualization of HRV, the heart rate is calculated by timing the interval between two consecutive heart beats and plotted against ECG signal.

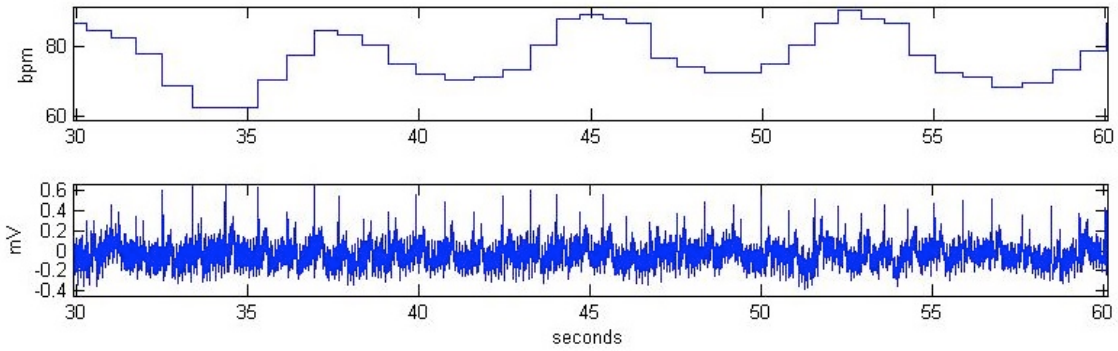

Figure 18: Heart rate between adjacent heartbeats

4. Results and Discussion

As mentioned in the previous chapter, the $\Delta Z / Z_0$ ratio did not provide a significant difference across different frequencies, therefore the resulting figures from each frequency are visually inspected and 30 kHz is decided as an appropriate frequency for the rest of the investigation. The output for 30 kHz can be seen below with all signa, and all results across frequencies can be found in appendix A in its entirety.

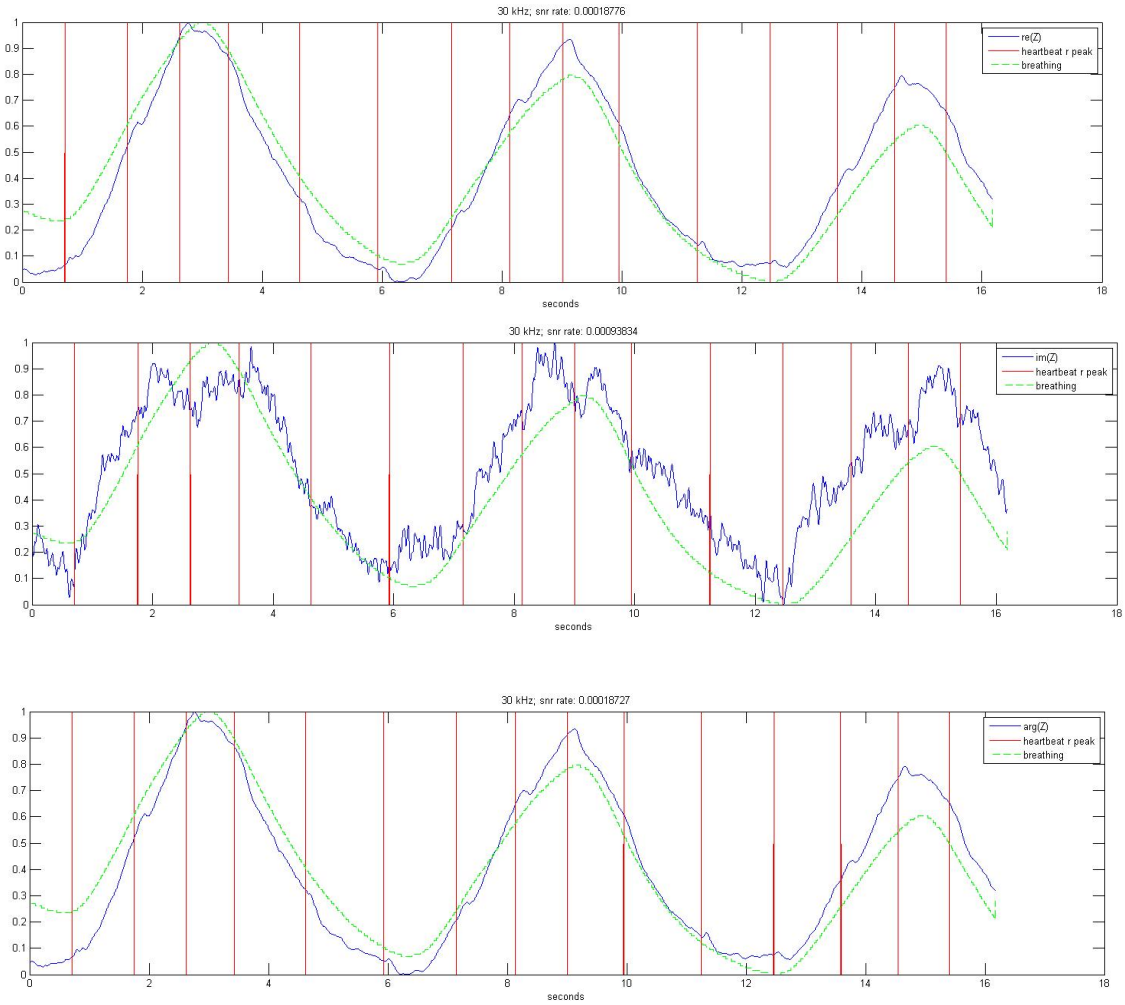

Figure 19: Real part, imaginary part and magnitude of Z at 30 kHz, respectively

It can be seen that bioimpedance signal dips slightly after every heartbeat as expected. The correlation between bioimpedance signal and respiration is also clearly noticeable.

As mentioned in chapter 3, reducing the sampling rate introduced some noise into the ECG signal obtained and this caused the R peaks to be harder to pick on some portions of the data. An example can be seen in figure 20, where there are multiple peaks

introduced by the noise and R peaks are hard to distinguish.

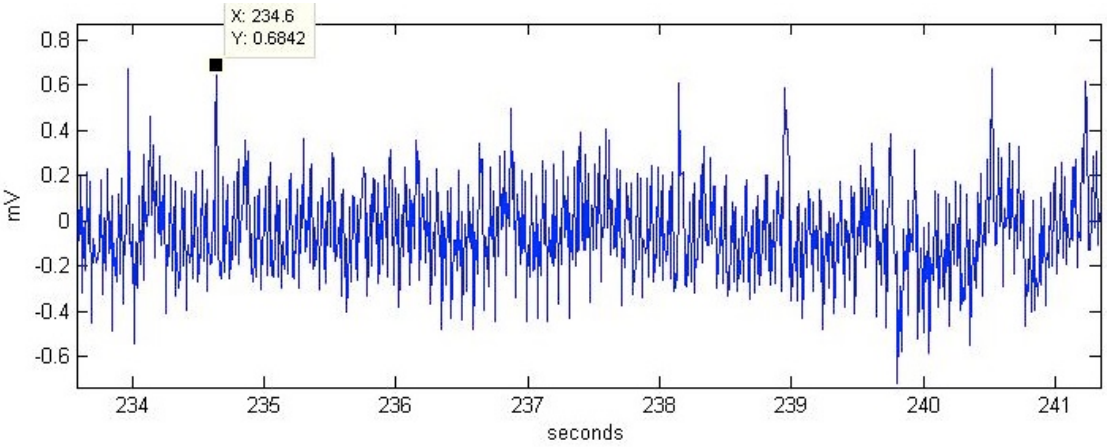

Figure 20: Few possible candidates for the next R peak

Even with this ambiguity present, candidates for R peaks are picked and corresponding locations on the impedance data are examined. As noted in section 2.2, impedance is expected to have a negative dip just after each R peak. The following figure demonstrates a portion of the ECG data with 2 possible locations, and examination of the correspondent points on the impedance data.

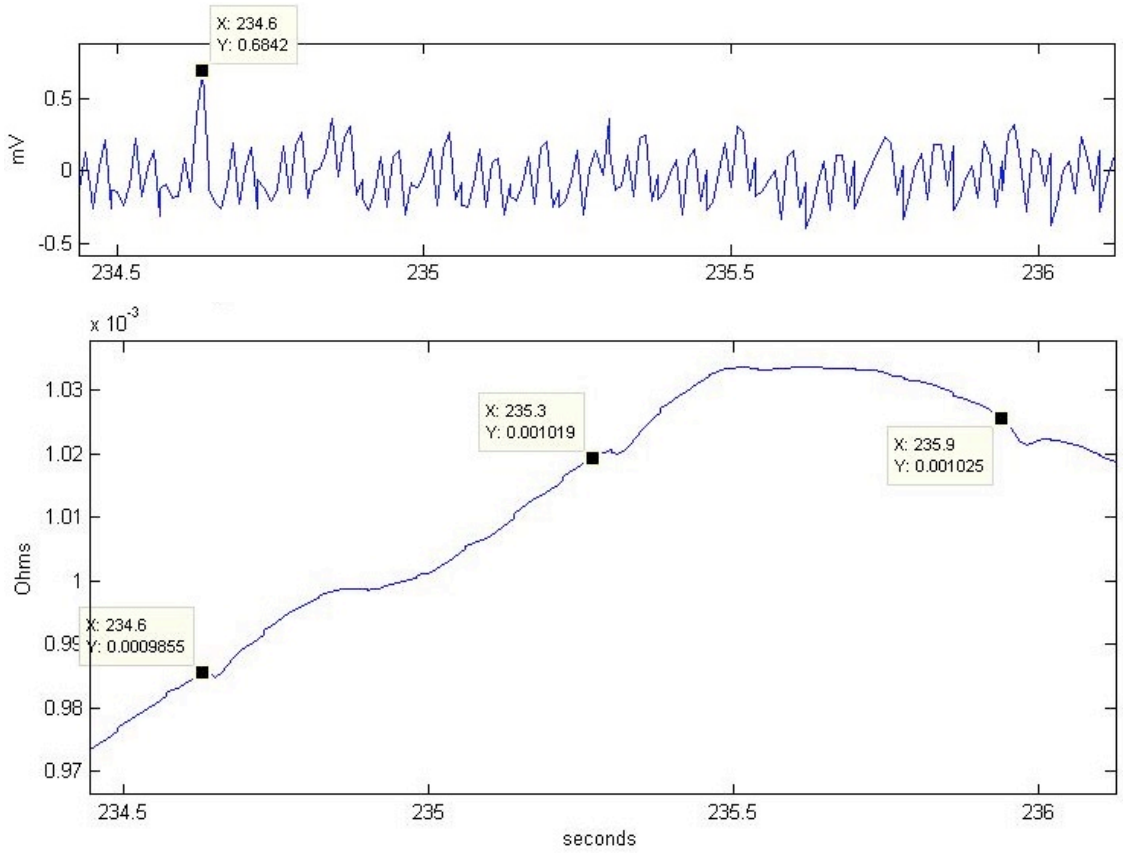

Figure 21: Ambiguous position of R peak and examination of the exact location from impedance

After all the R peaks are marked on ECG data, EBI signal is also inspected and negative dips are marked for sake of comparison. When compared element by element, points taken from EBI data have a difference with a mean of 20,6ms, and a standard deviation of 10ms. This is expected, since the bioimpedance keeps decreasing for a short duration after the R peak as explained in section 2.2.

As mentioned in previous chapter, respiration data is also affected from reduction of sampling rate and has a trend that at first decreases and then increases. Still, the local maxima, which correspond to transitions between inhaling and exhaling, are assumed to be in realistic locations on the time axis. To remove the trend from respiration data, a simple running average is calculated with a window size of 2000 points and subtracted from the actual breathing data.

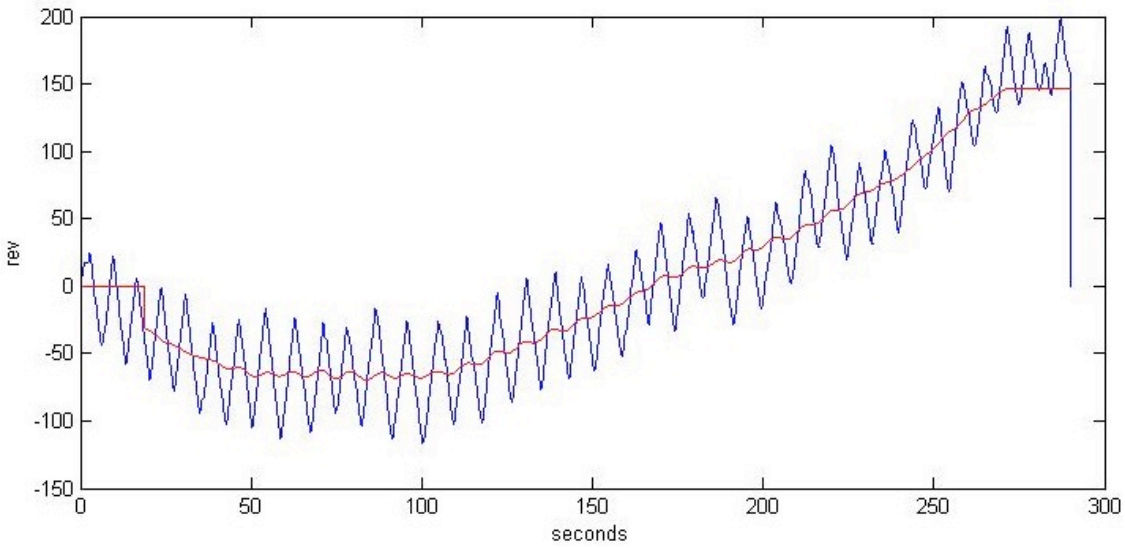

Figure 22: Respiration signal and running average over 2000 points

Bioimpedance signal is expected to be directly correlated with respiration. Even though the relationship is observable by visual inspection, the cross correlation function between EBI and detrended respiration signal is plotted below. It is worth noting that autocorrelation between these two signals is at its maximum around 0, meaning that there is maximum overlap when there is no delay. This implies that given an appropriate method for extraction, respiration information can be extracted directly from bioimpedance signal

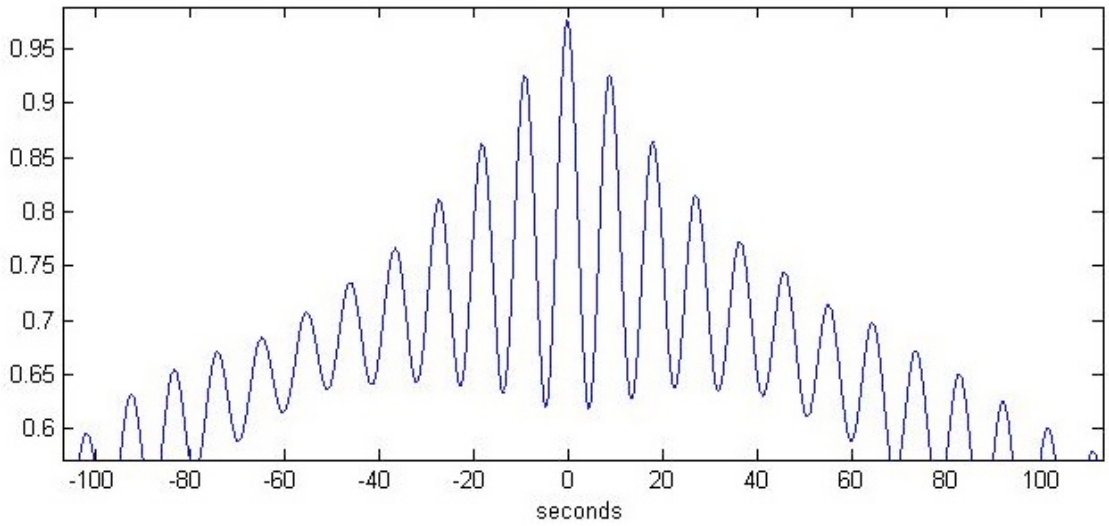

Figure 23: Correlation of bioimpedance and respiration

When the heart rate is plotted with detrended respiration signal, the relationship between respiration and heart rate is also apparent. Although heart rate seems to

increase with inhalation and decreases with exhalation, they are not perfectly in-phase with each other. This is believed to be due to respiratory pacemaker oscillations in the central nervous system[13]. It is also suggested that this phase difference can be influenced with paced respiration[13].

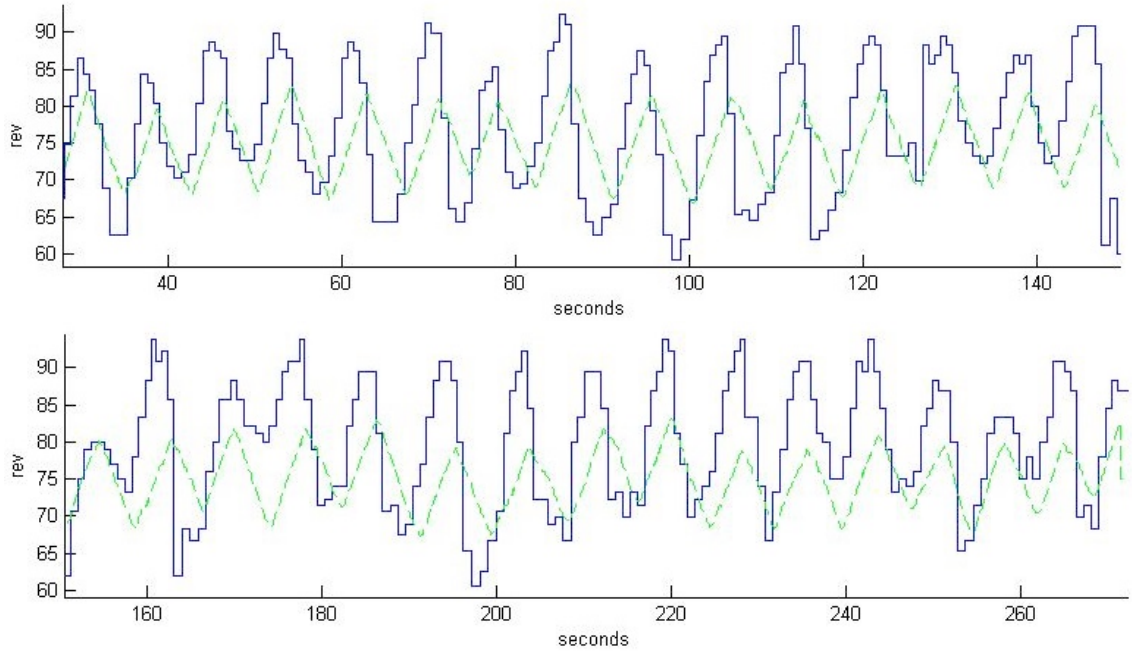

Figure 24: Heart rate (continuous) and respiration (dashed)

To sum up, bioimpedance signal is found to contain both heartbeat and respiration information accurately. The obtained data also coincides with previous findings. Upon development of methods for successful extraction of respiration and cardiac data, suggested setup is promising for investigation of the influence of respiration on heart rate variability.

5. Conclusions

At first glance, respiratory and cardiac components in bioimpedance signal appear to be visually distinguishable. The intuition to design a low-pass filter for acquiring the respiratory component and a high pass filter for the cardiac component seems plausible. This approach has a chance to work for the data presented in this thesis, however, when thought that the main objective is to analyze the influence of one component on the other, especially for diagnostic purposes, it is also apparent that it will fail when these two components get close to each other in frequency spectrum.

As the previous work suggested, the development of known methods are not suitable for solving the task of effective separation of the cardiac and respiratory components of bioimpedance signal, and therefore new methods need to be developed [4]. This thesis confirms that electrical bioimpedance is a good candidate for investigation of the relationship between breathing and heart beat variability, though a method for separation of cardiac and respiratory components are needed.

It is known that heart rate variability and respiration are valuable tools for diagnosis for certain pathologies. 24 hours of monitoring of these information is also an important input. With this information in mind, portable devices for long duration monitoring would be a valuable tool for diagnosis. In case of successful extraction of relevant data, biggest obstacle for achieving this is the size of the impedance spectroscope and current source. In presence of a portable device containing both a current source and an impedance spectroscope, the rest of the setup can be implemented as a wearable device.

References:

1. Committee on Military Nutrition Research; Institute of Medicine, "Emerging Technologies for Nutrition Research: Potential for Assessing Military Performance Capability":170-1, National Academies Press, Washington (DC), USA, 1997
2. Hinton A.J. and SayersB., "Advanced Instrumentation for Bioimpedance Measurements", Solartron, Victoria Rd., Farnborough, Hampshire UK, , 1998.
3. Min M., Kink A., Land R., Parve T., and Rätsep I., "Modification of Pulse Wave Signals in Electrical Bioimpedance Analyzers for Implantable Medical Devices", Proceedings, Conference of the IEEE EMBS., San Francisco, CA, USA, 2004.
4. Krivosei A., "Model Based Method for Adaptive Decomposition of the Thoracic Bio-impedance Variations into Cardiac and Respiratory Components", Tallinn University of Technology, Tallinn, Estonia, 2009
5. Kleiger RE, Miller JP, Bigger JT Jr, Moss AJ. "Decreased heart rate variability and its association with increased mortality after acute myocardial infarction", American Journal of Cardiology, 59 (4): 256 – 262, 1987
6. Malik M. et al., "Heart rate variability: standards of measurement, physiological interpretation, and clinical use", European Heart Journal (1996) 17, 354–381
7. Hirsh JA, Bishop B. "Respiratory sinus arrhythmia in humans; how breathing pattern modulates heart rate". American Journal of Physiology 1981; 241: H620–9.
8. http://www.zhinst.com/
9. S. Grimnes, Ø.G. Martinsen, Bioimpedance and Bioelectricity Basics, Academic Press, 2008.
10. Samieipour A., "Thoracic Bioimpedance Measurement", Tallinn University of Technology, Tallinn, Estonia, 2013
11. Seppa V.P. et al, "Novel electrode configuration for highly linear impedance pneumography", Biomedizinische Technik 01/2013; 58(1):35-8, 2013.
12. Malmivuo J, Plonsey R, "Bioelectromagnetism: Principles and Applications of Bioelectric and Biomagnetic Fields" Oxford University Press, Oxford, 1995
13. Lehrer P, Gevirtz R, "Heart rate variability biofeedback: how and why does it work?", Frontiers of Psychology, 5:756, 2014

Appendix A: MATLAB codes for implementation

```
function editdata (A)

%Takes the measurement matrix and converts 8 channels
%of real and imaginary parts to 8 vectors of magnitudes
%also extracts timestamp and ecg signals

assignin('base','timestamp',A(3:end,1));

[th1,r1]=cart2pol(A(3:end,2),A(3:end,3));
assignin('base','f1',r1);
[th2,r2]=cart2pol(A(3:end,4),A(3:end,5));
assignin('base','f2',r2);
[th3,r3]=cart2pol(A(3:end,6),A(3:end,7));
assignin('base','f3',r3);
[th4,r4]=cart2pol(A(3:end,8),A(3:end,9));
assignin('base','f4',r4);
[th5,r5]=cart2pol(A(3:end,10),A(3:end,11));
assignin('base','f5',r5);
[th6,r6]=cart2pol(A(3:end,12),A(3:end,13));
assignin('base','f6',r6);
[th7,r7]=cart2pol(A(3:end,14),A(3:end,15));
assignin('base','f7',r7);
[th8,r8]=cart2pol(A(3:end,16),A(3:end,17));
assignin('base','f8',r8);

assignin('base','ecg',A(3:end,18));
end
```

```
function makegrid(peaks)

%this function takes the r-peak locations and
%outputs a grid with unitary triangles there

l = evalin('base', 'length(ecg)');
g=zeros(l,1);

for i=1:length(peaks);
    g(peaks(i))=0;
    g(peaks(i)+1)=1;

end
assignin('base','grid',g);
end
```

```
function ecgcomp(data)

%this function takes a data vector as input and
%plots it together with the information already
%present in base workspace such as ecg breathing and time
%it also calculates the ratio of variation
%of the input to its mean

grid=evalin('base', 'grid');
timestamp=evalin('base', 'timestamp');
breathe=evalin('base','breathing');
f=evalin('base','current_frequency');
l=length(timestamp);


%running average for smoothing the curve
%trend is running average and small is difference
window=40;
for i=window+1:(l-window-1)
    trend(i)=sum(data(i-window:i+window))/(2*window+1);
    small(i)=trend(i)-data(i);
end

%get rid of zero padding in beginning

 trend(1:window)=trend(window+1:2*window);
 %calculate RMS values
 rms_main=rms(data);
 rms_small=rms(small);
 rms_ratio=rms_small/rms_main;

    %plots for diagnostics
    % figure
    % plot(data)
    % hold on
    % plot(trend,'r')
    %
    % figure
    % plot(small)


 %normalize for plotting
 normal_data=(data-min(data))/(max(data)-min(data));
 normal_breathe=(breathe-min(breathe))/(max(breathe)-min(breathe));



figure
plot(timestamp,normal_data);
hold on
%axis ([0 max(timestamp) min(data) max(data)])
plot(timestamp,grid,'r')
plot(timestamp,normal_breathe,'--g')
title([num2str(f/1000) ' kHz; snr rate: ' num2str(rms_ratio)])
xlabel('seconds')
legend('re(Z)','heartbeat r peak','breathing')

end
```

```
function extractfifth (A)

%this function takes the measurement matrix as input and gives following
%vectors as output: real part, imaginary part, magnitude of impedance
%as well as ecg, breathing, timestamp.
%it also prints out the frequency of which the data is collected

time=A(3:end,1);
real=-A(3:end,10);%reverse electrode locatons
imag=-A(3:end,11);%reverse electrode locatons
ecg=A(3:end,18);
spiro1=A(3:end,20);
spiro2=A(3:end,21);


[th5,r5]=cart2pol(real,imag);
l=length(time);




%calculate breathing

for i=1:l-1
    if (spiro1(i)==0&&spiro2(i)==0)
        spirodiff(i+1)=spiro1(i+1)-spiro2(i+1);
    end
end
breathe=cumsum(spirodiff);
breathe(l)=0;



assignin('base','fmagn',r5);
assignin('base','freal',real);
assignin('base','fimag',imag);
assignin('base','ecg',ecg);
assignin('base','breathing',breathe);
assignin('base','timestamp',time);
assignin('base','current_frequency',A(1,10));

end
```

```
function heartrate
timestamp=evalin('base', 'timestamp');
breathe=evalin('base','breathing');
grid=evalin('base', 'grid');
Rpeaks=evalin('base','Rpeaks');
ecg=evalin('base', 'ecg');

l=length(timestamp);
b=length(Rpeaks);
pulses=timestamp(Rpeaks);
dt=diff(pulses);
HR=60./dt;
HR(b)=mean(HR);


figure
subplot(2,1,1)
stairs(pulses,HR)
subplot(2,1,2)
plot(timestamp,ecg)
```

```
function fixbreathe
timestamp=evalin('base', 'timestamp');
breathe=evalin('base','breathing');

l=length(breathe);

%running average for smoothing the curve
%trend is running average and small is difference

small=zeros(1,l);
window=2100;
for i=window+1:(l-window-1)
    trend(i)=sum(breathe(i-window:i+window))/(2*window+1);
    small(i)=breathe(i)-trend(i);
end

assignin('base','breathing_fixed',small);
```

Appendix B: Obtained Data

Following are the outputs of first 5 measurements. Channels 5, 6, 7 and 8 are used with .2 times the maximum amplitude to avoid any clipping.

Measurement 1:

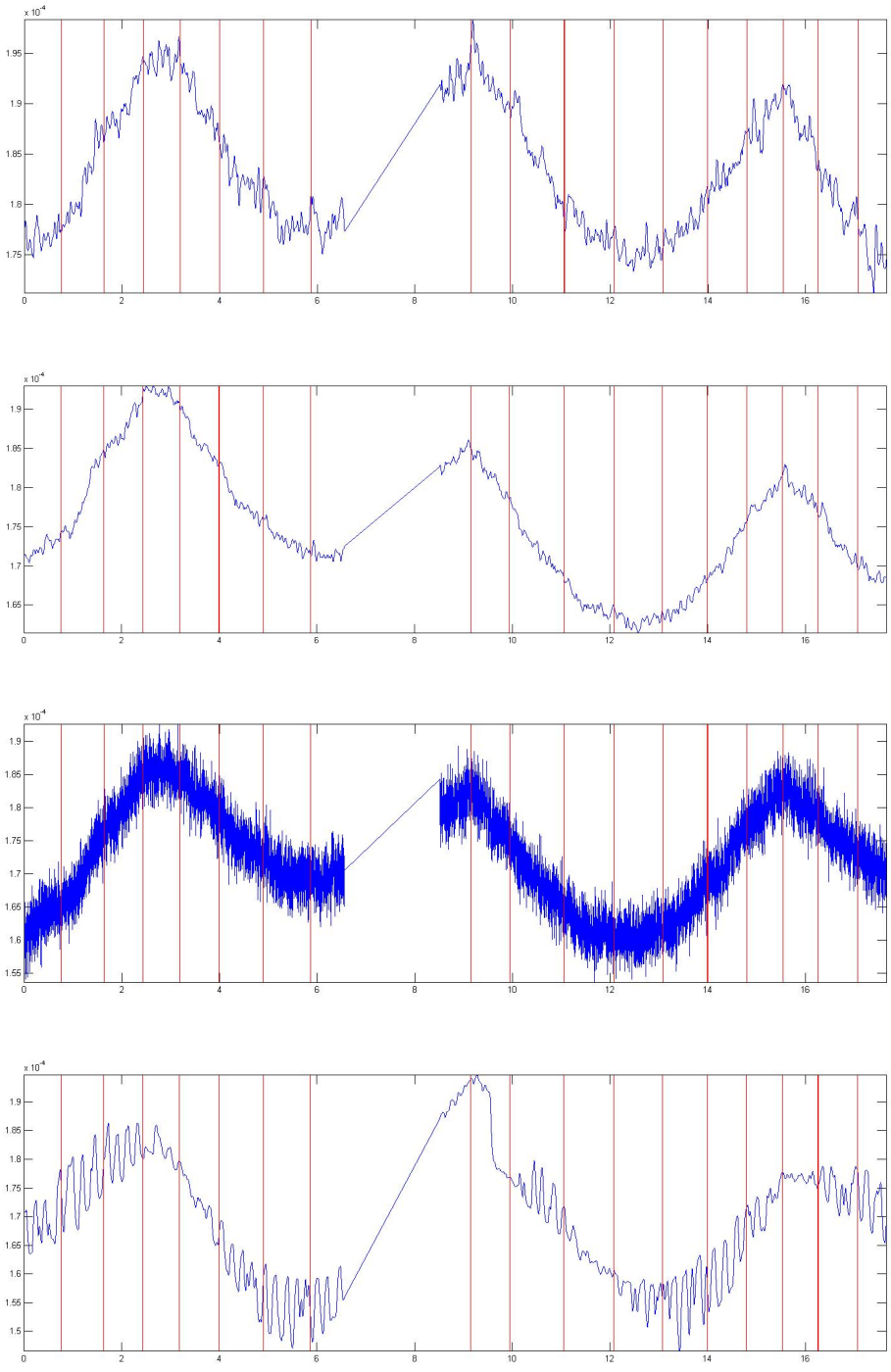

Figure 25: Magnitude of Z for 1, 3, 5 and 8 kHz, respectively

Measurement 2:

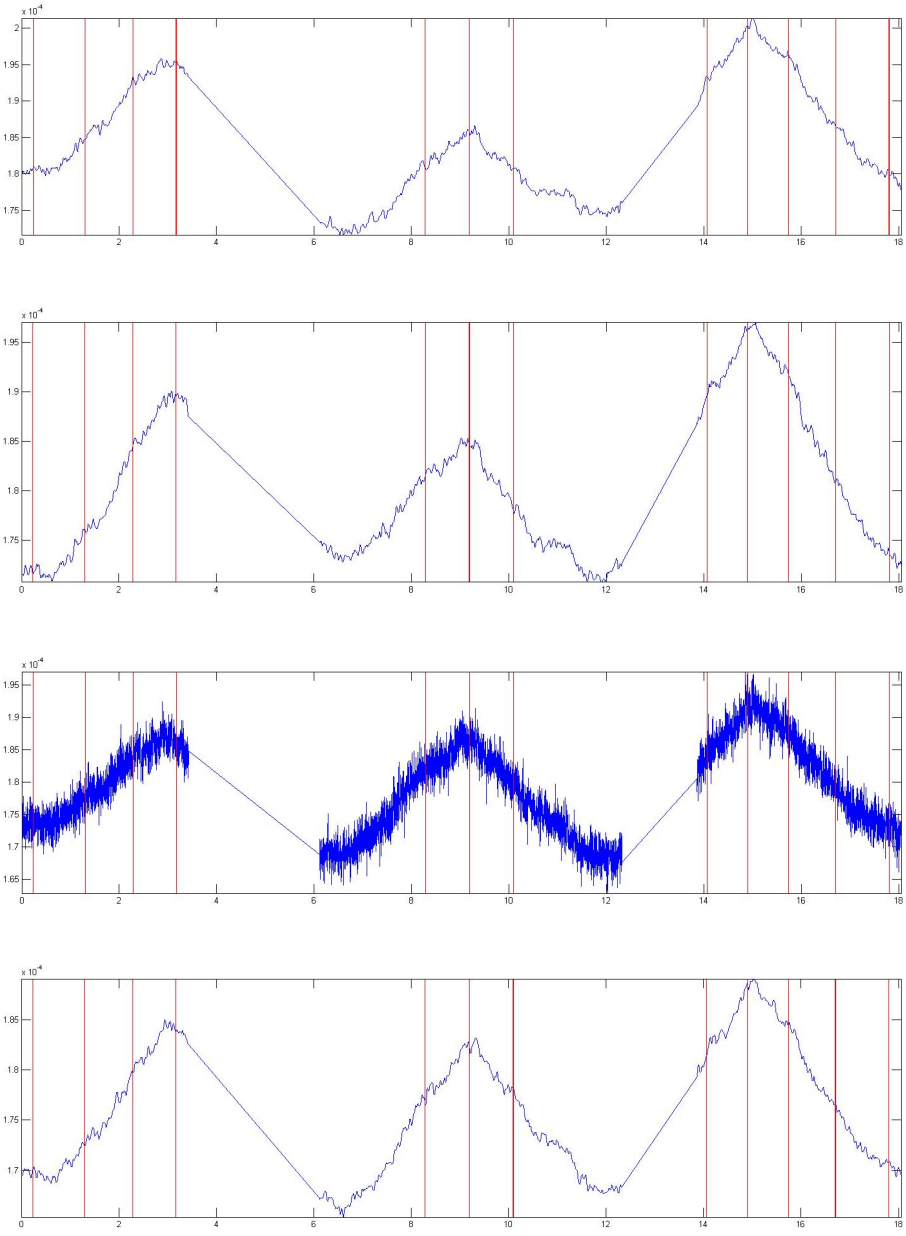

Figure 26: Magnitude of Z at 5, 7, 9 and 11 kHz, respectively

Measurement 3:

As seen in previous measurements, seventh channel is problematic for some reason. From here on, it is omitted, and an amplitude of .3 times the maximum is used.

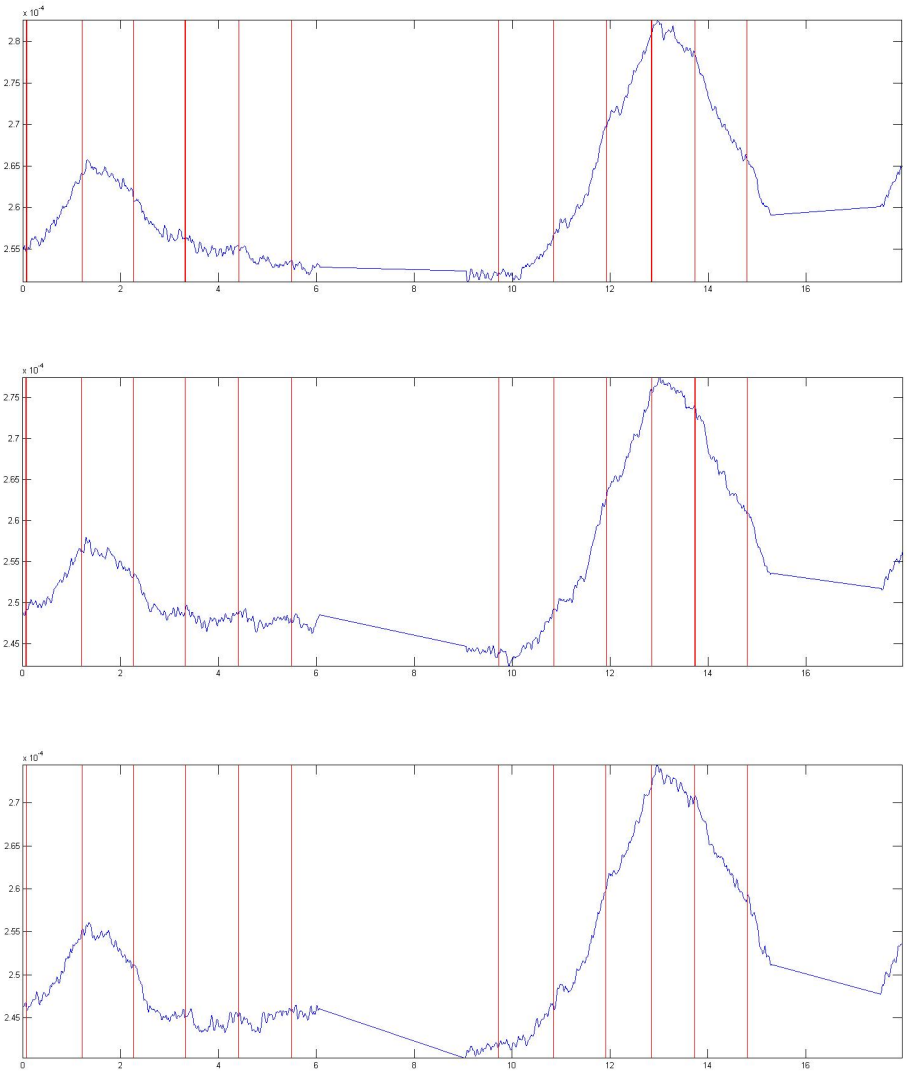

Figure 27: Magnitude of Z at 9, 13 and 15 kHz, respectively

Measurement 4:

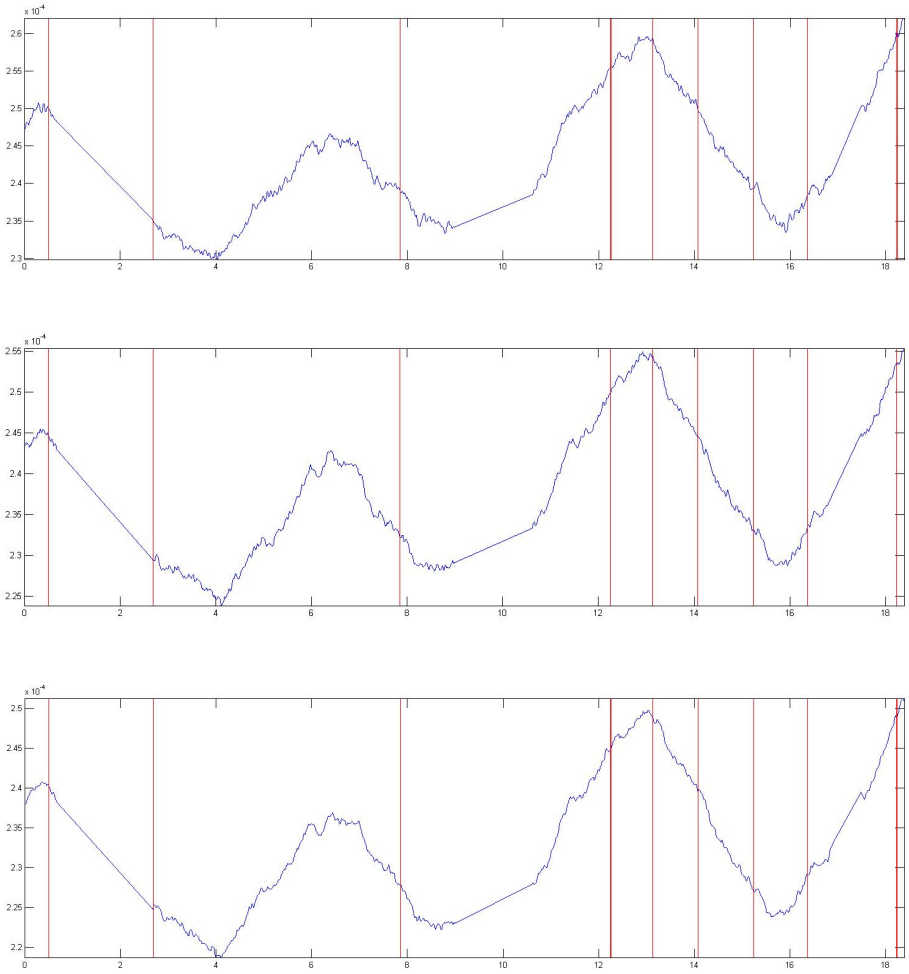

Figure 28: Magnitude of Z at 20, 25 and 30 kHz, respectively

Measurement 5:

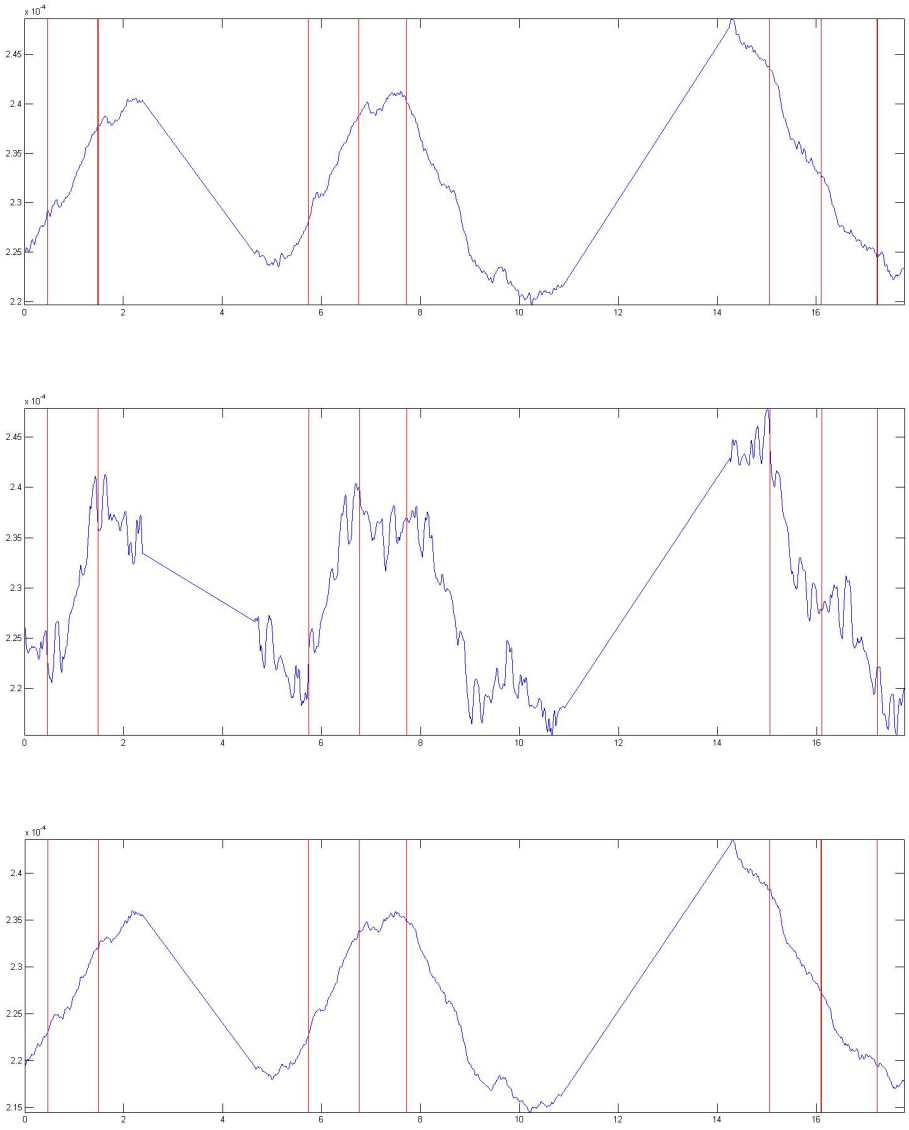

Figure 29: Magnitude of Z at 35, 40 and 45 kHz, respectively

It is noted that these outputs are inadequate and the setup is reviewed. With minor changes in software, and using only one channel with maximum amplitude, the following outputs are obtained

Measurement 6: 1 kHz

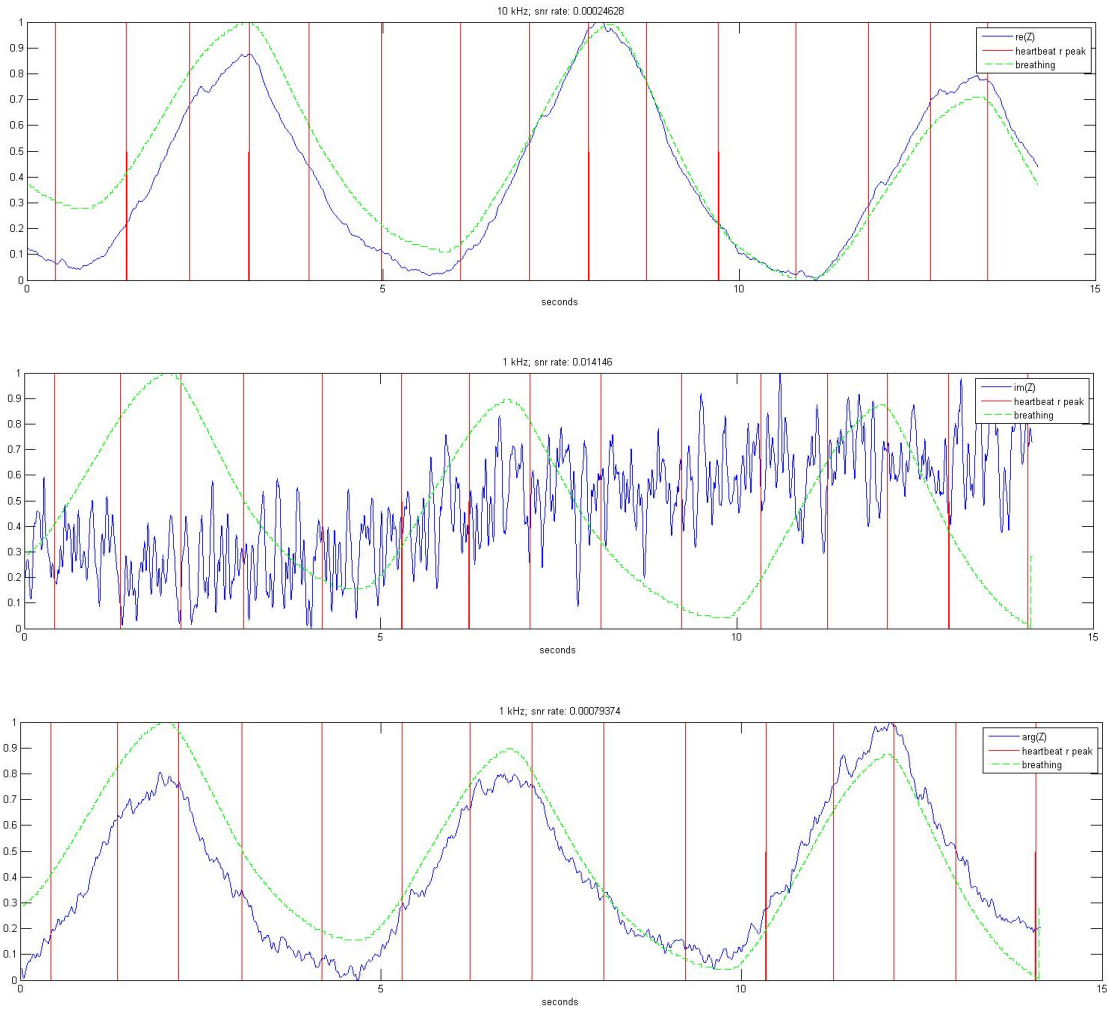

Figure 30:Real part, imaginary part and magnitude of Z at 1kHz

Measurement 7: 5 kHz

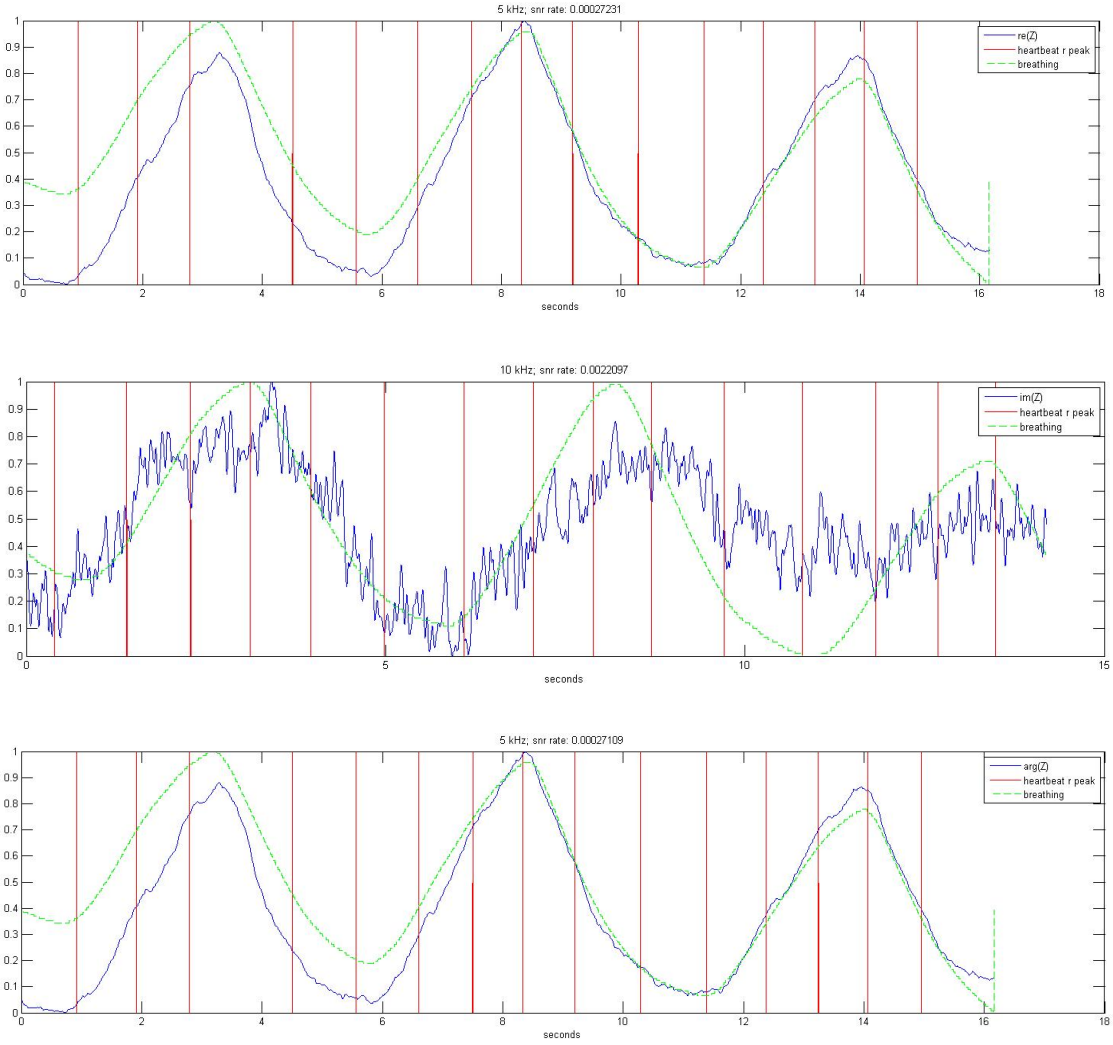

Figure 31:Real part, imaginary part and magnitude of Z at 5 kHz

Measurement 8: 10 kHz

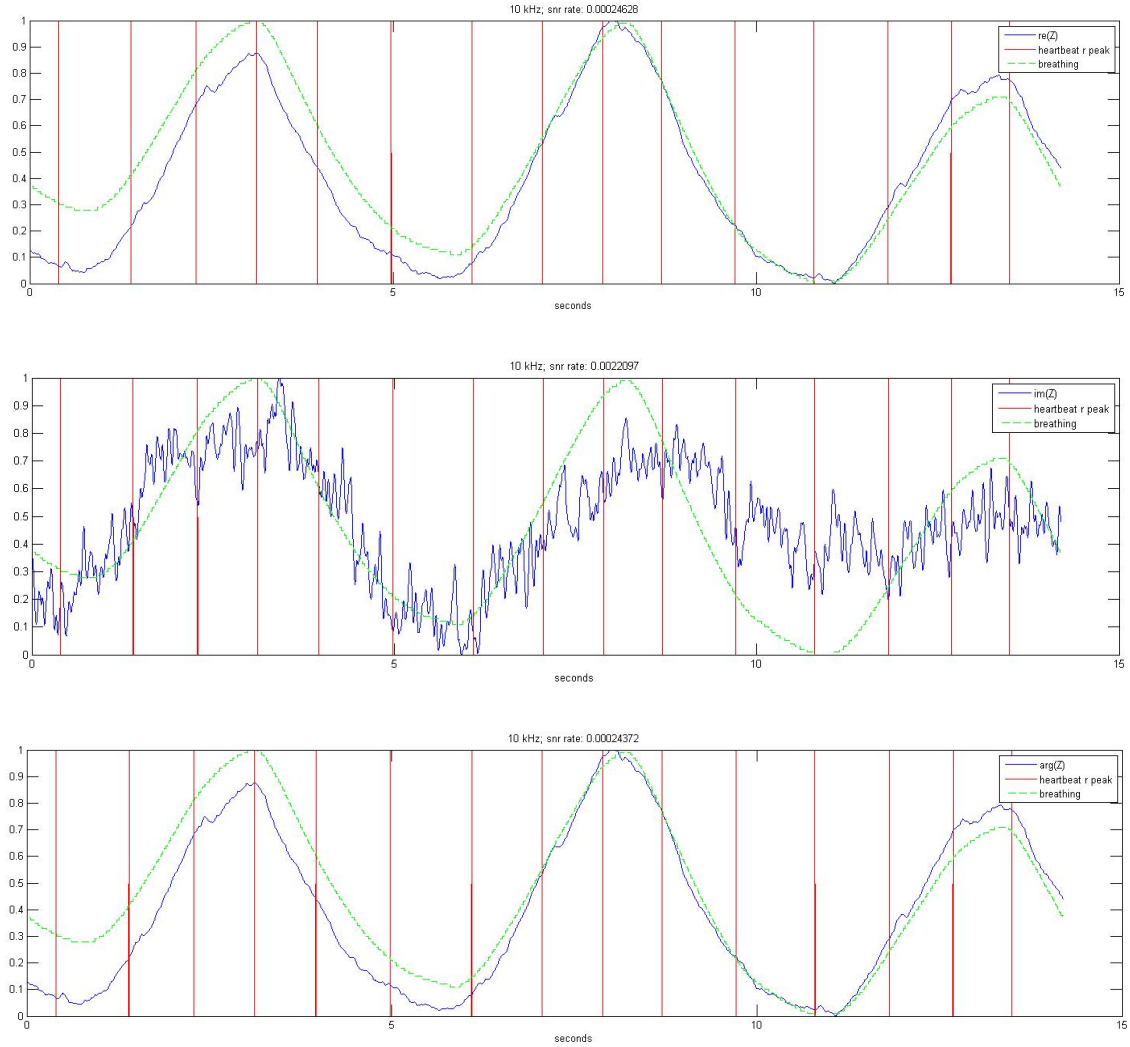

Figure 32:Real part, imaginary part and magnitude of Z at 10kHz

Measurement 9: 15 kHz

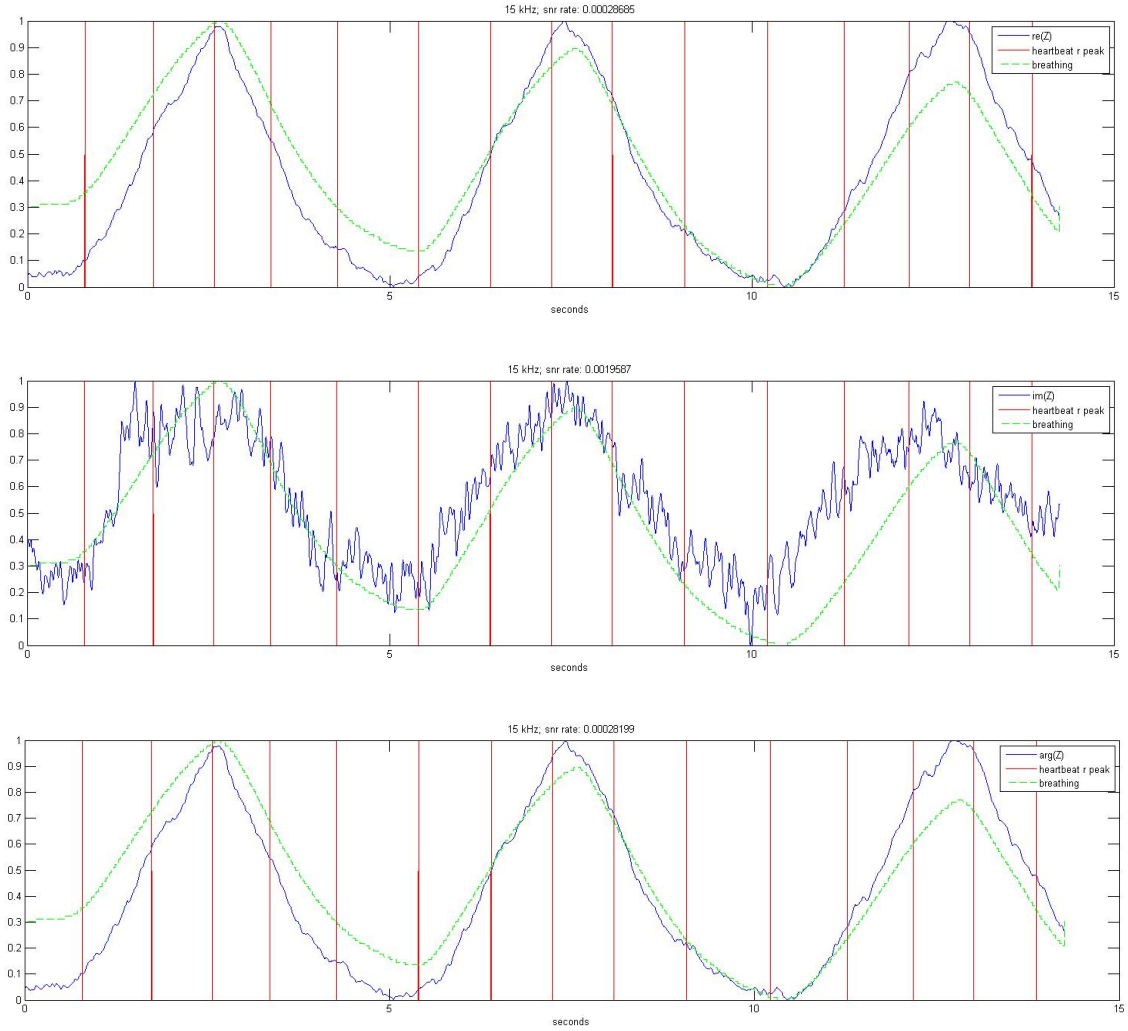

Figure 33:Real part, imaginary part and magnitude of Z at 15 kHz

Measurement 10: 20 kHz

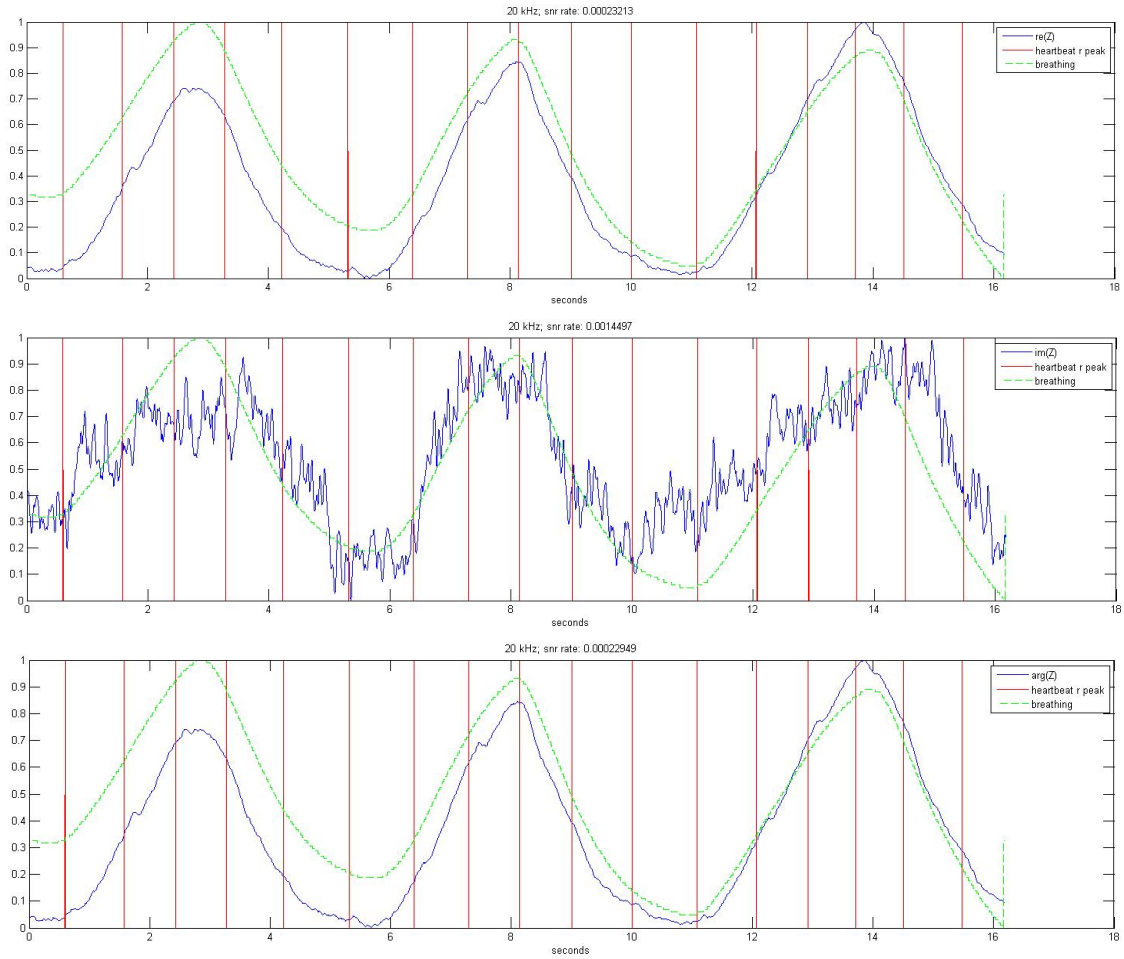

Figure 34: Real part, imaginary part and magnitude of Z at 20 kHz

Measurement 11: 25 kHz

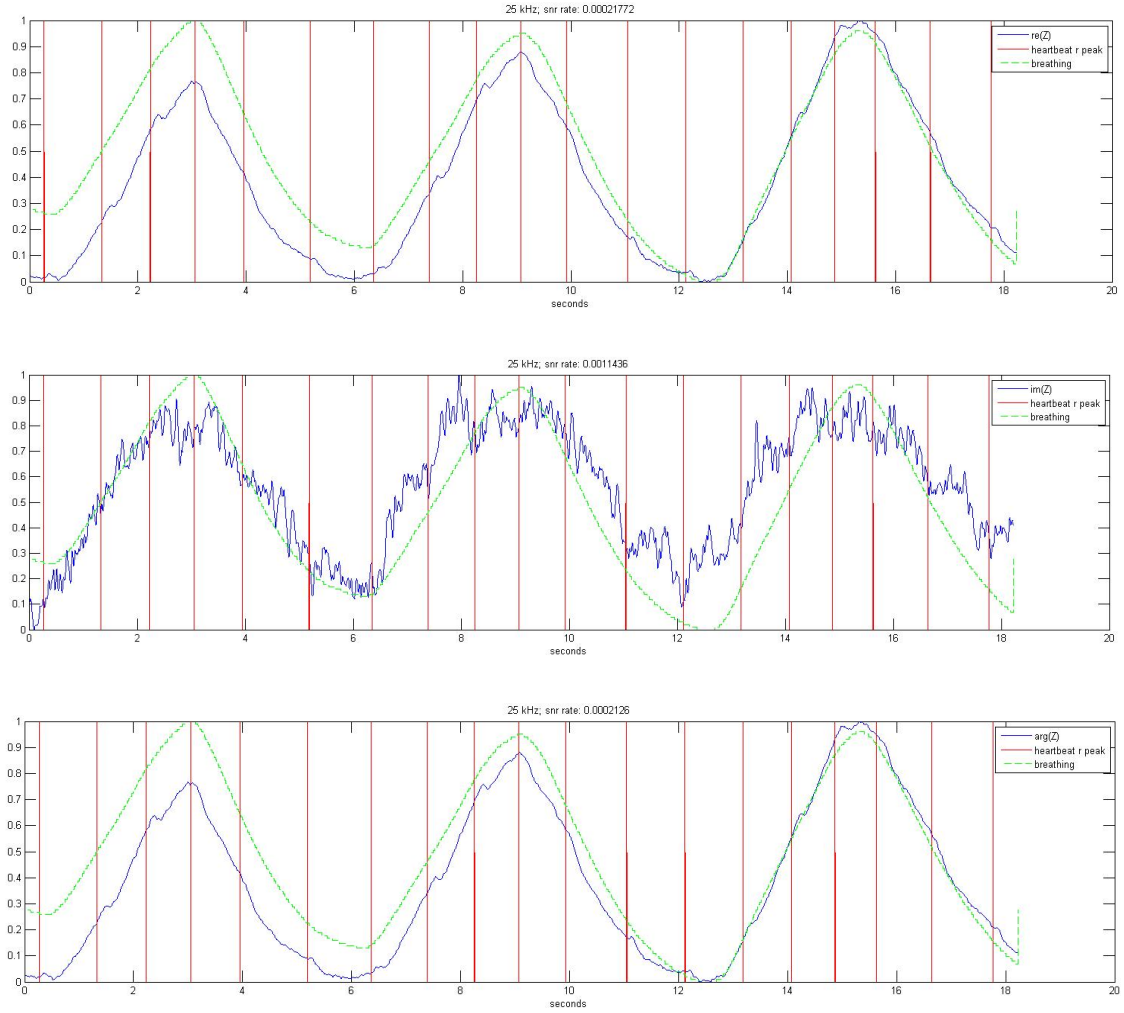

Figure 35:Real part, imaginary part and magnitude of Z at 25 kHz

Measurement 12: 30 kHz

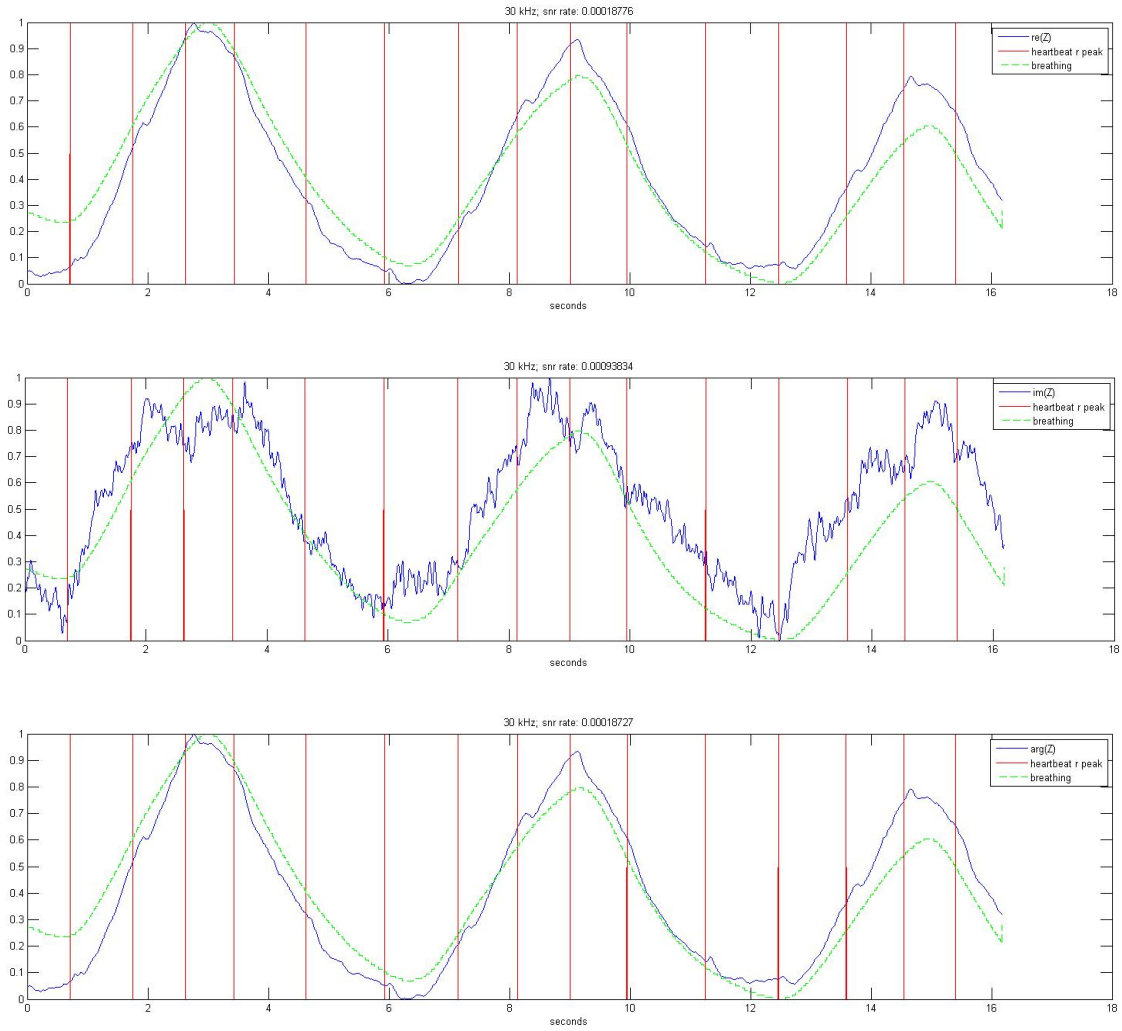

Figure 36: Real part, imaginary part and magnitude of Z at 30 kHz

Measurement 13: 35 kHz

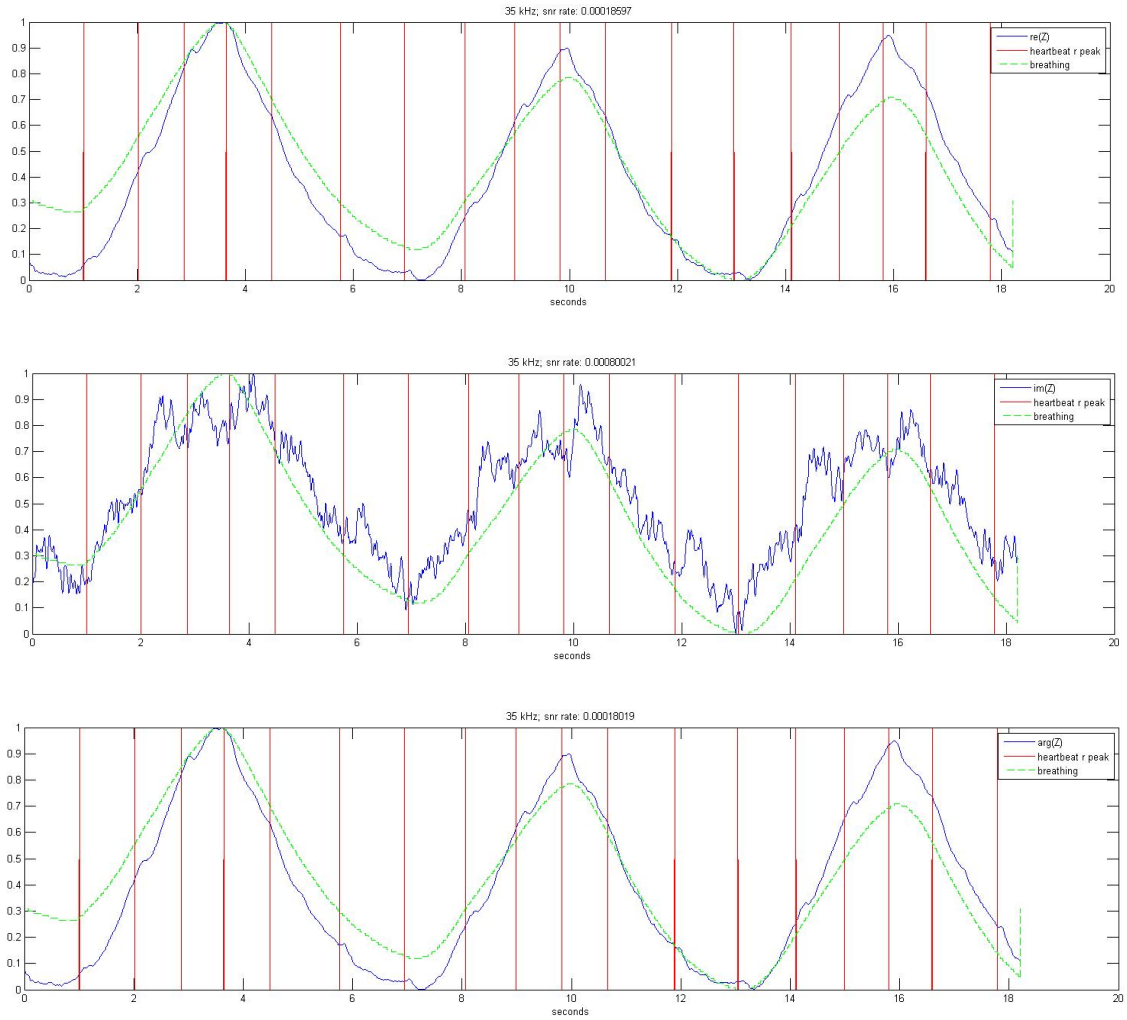

Figure 37: Real part, imaginary part and magnitude of Z at 35 kHz

Measurement 14: 40 kHz

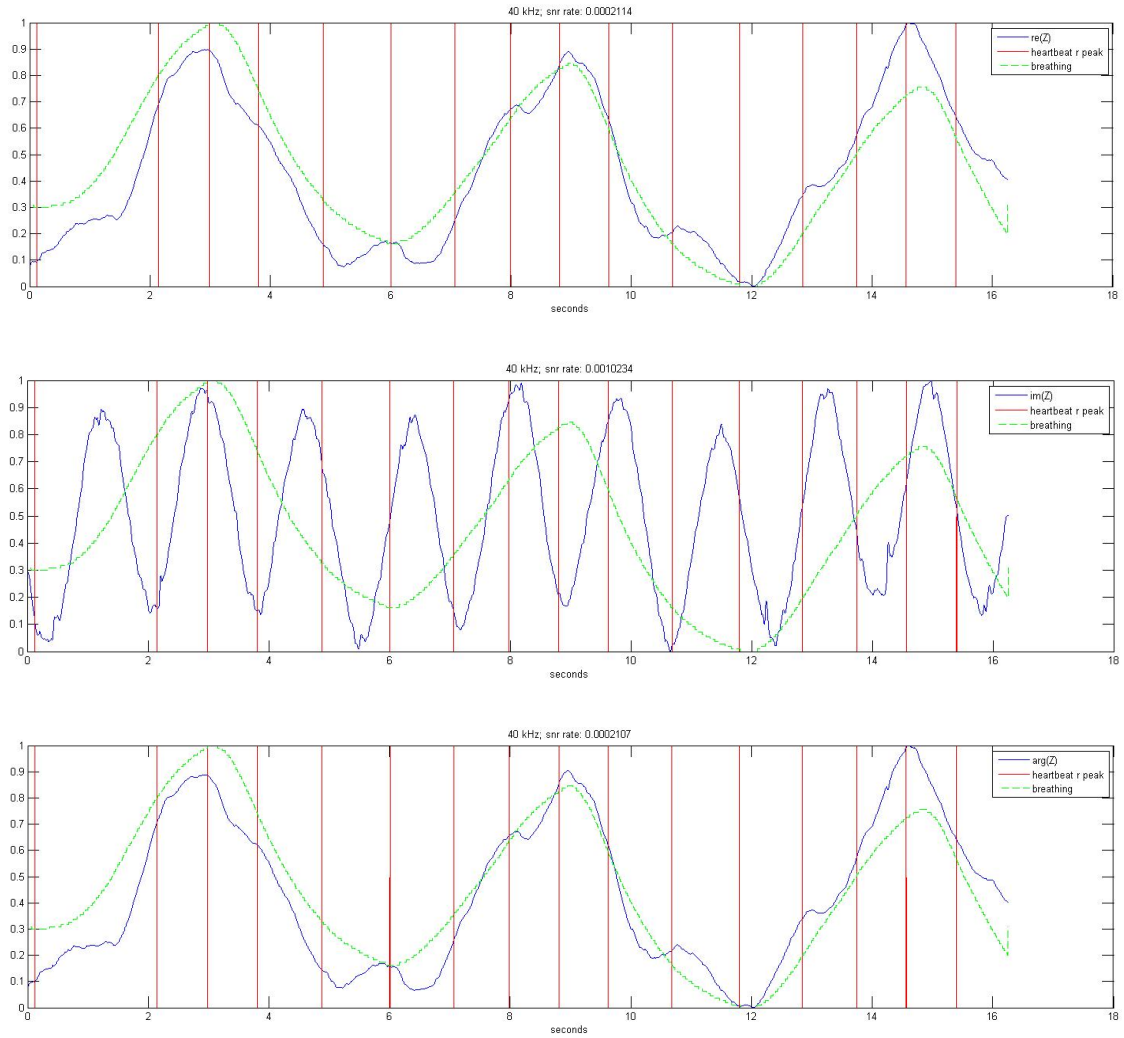

Figure 38: Real part, imaginary part and magnitude of Z at 40 kHz

Measurement 15: 45 kHz

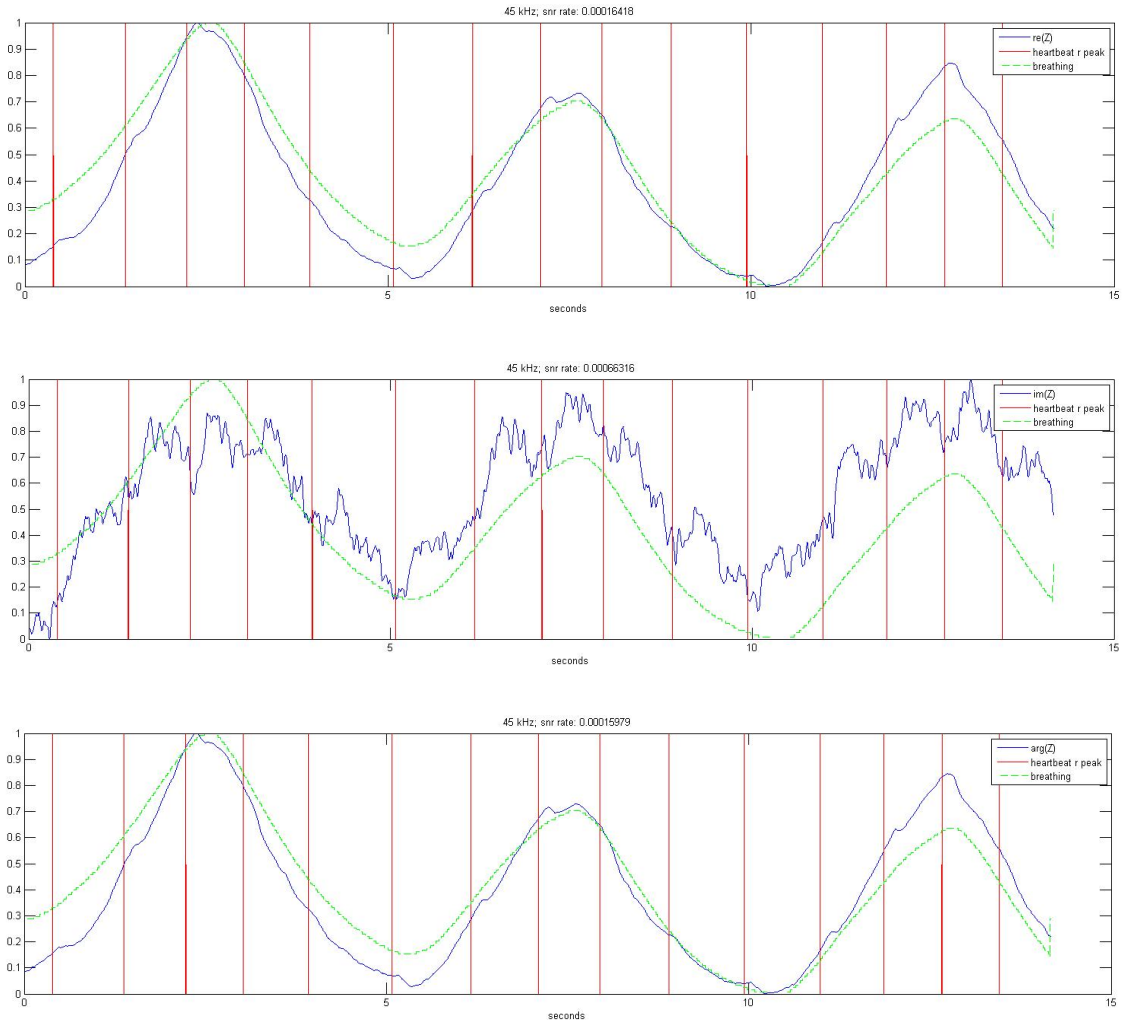

Figure 39: Real part, imaginary part and magnitude of Z at 45 kHz

Measurement 16: 50 kHz

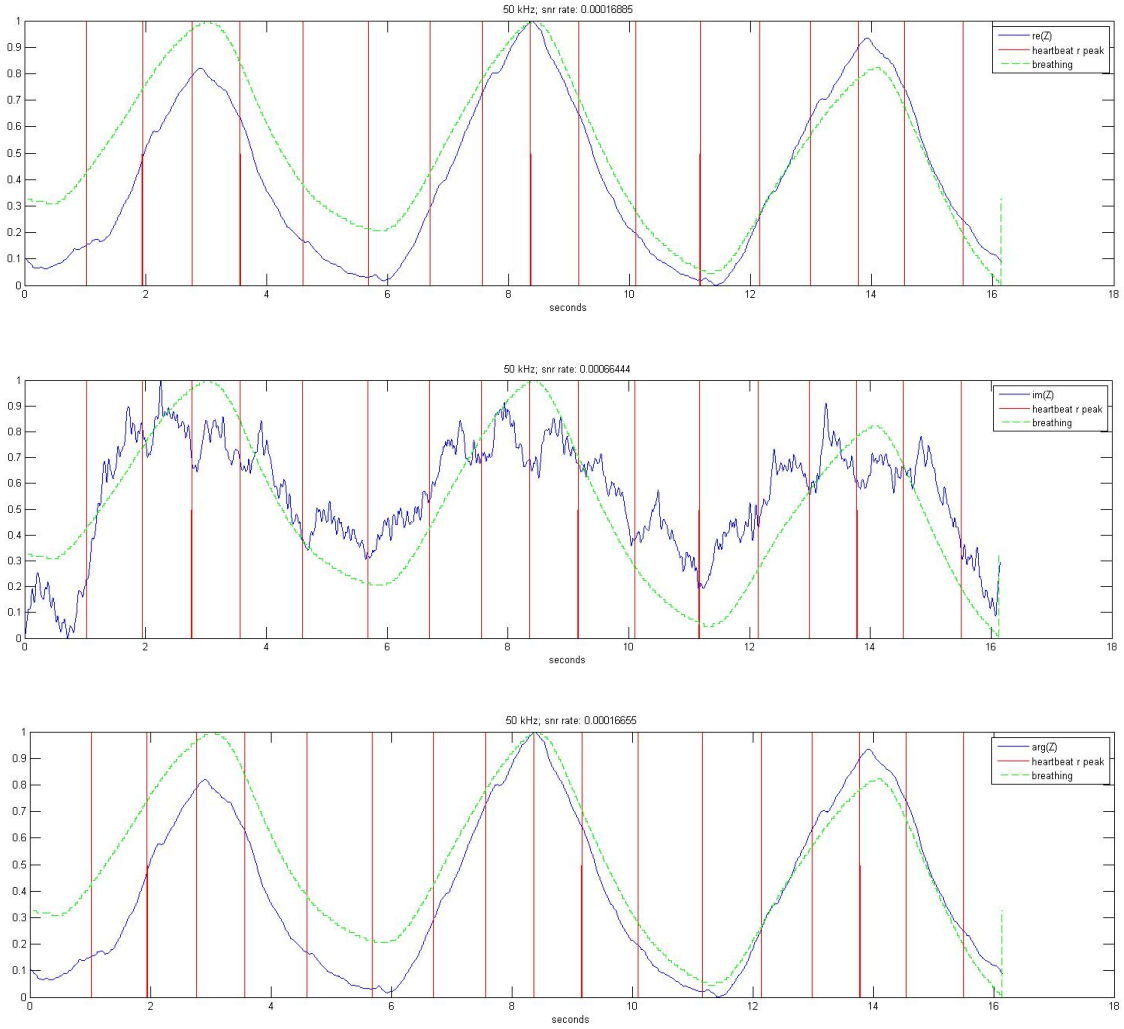

Figure 40: Real part, imaginary part and magnitude of Z at 50 kHz